Research Laboratory
of the
Portland Cement Association

BULLETIN 11

Shrinkage Stresses in Concrete

Part 1—Shrinkage (or Swelling), Its Effect upon Displacements and Stresses in Slabs and Beams of Homogeneous, Isotropic, Elastic Material

Part 2—Application of the Theory Presented in Part 1 to Experimental Results

By
GERALD PICKETT

MARCH, 1946

CHICAGO

Authorized Reprint from Copyrighted
JOURNAL OF THE AMERICAN CONCRETE INSTITUTE
New Center Building, 7400 Second Boulevard
Detroit 2, Michigan
Jan. and Feb. 1946, PROCEEDINGS *Vol. 42, pp. 165-204 and 361-400*

Title 42-8 —a part of PROCEEDINGS, AMERICAN CONCRETE INSTITUTE Vol. 42

JOURNAL
of the
AMERICAN CONCRETE INSTITUTE
(copyrighted)

Vol. 17 No. 3 7400 SECOND BOULEVARD, DETROIT 2, MICHIGAN January 1946

Shrinkage Stresses in Concrete*

By GERALD PICKETT†
Member American Concrete Institute

SYNOPSIS

Theoretical expressions for deformations of concrete beams and slabs that occur during the course of drying and expressions for distribution of the accompanying shrinkage stresses are derived in Part 1. These expressions are derived on the assumption that the laws governing the development of shrinkage stresses in concrete during drying are analogous to those governing the development of thermal stresses in an ideal body during cooling. Three cases are considered:

(a) slab or beam drying from one face only;
(b) slab or beam drying from two opposite faces; and
(c) prism drying from four faces.

The applicability of the equations to concrete is considered in Part 2 (to appear ACI JOURNAL, February 1946). It is shown that the course of shortening of prisms is in very good agreement with the theoretical equations and that from a test on one prism the shortening versus period of drying of other prisms of the same material differing in size and number of sides exposed to drying can be predicted with fair accuracy if the differences in size are not too great. However, it is shown that the theory must be modified to take into account inelastic deformation and to permit the supposed constants of the material to vary with moisture content and size of specimen if the theory is to be in agreement with all results on all types of specimen of a given concrete.

Various tests are described which, when used in conjunction with the theory, provide a means for studying some of the more fundamental properties of concrete and for predicting the performance of concrete under some conditions in the field.

INTRODUCTION

Concrete, like many other materials, gains or loses water with changes in ambient conditions. With each change in water content the concrete

*Received by the Institute, April 30, 1945.
†Professor of Applied Mechanics, Kansas State College, Manhattan, Kans.; formerly Portland Cement Association Research Laboratory, Chicago.

tends to shrink or swell. As a result of these changes in volume, stresses are produced that may affect the performance of the concrete structure concerned.

In the design of concrete structures some consideration is usually given to the possibility of subsequent shrinkage or swelling, but the computations for stresses usually include only the stresses produced by loads. The computations are made by means of formulas taken from the science of mechanics of materials and the computed stresses so obtained are compared with allowable stresses, considering the type of structure and location of the concrete in the structure. The basic assumptions for the formulas are that the material is homogeneous, isotropic, free from self-strain and obeys Hooke's law.

Concrete is not homogeneous; by nature it is heterogeneous, even including the binding medium itself, hardened cement paste. It is not isotropic. Factors such as sedimentation before hardening tend to destroy what isotropy there might have been. It does not obey Hooke's law except perhaps under instantaneous strains. It is not free from self-strain at any time; the hardened paste may be shrinking while the aggregate may be resisting a change in volume; the regions near the surface may be fairly dry and tending to shrink whereas those farther inward may be much wetter and tending to resist a reduction in volume. In addition, concrete may change with time, becoming stronger and more rigid if conditions are such as to promote additional hydration.

Not only is concrete a much different material from that assumed in the derivations of elementary formulas but the conditions of loading, the tendency toward redundancy (statically indeterminate), and the structural shapes of concrete members are often such as to make the elementary formulas only rough approximations compared with what the same formulas would be for the usual conditions of loading and structural shapes of steel structures which are usually less redundant.

It is not to be inferred that concrete would necessarily be a better material were all of its properties like those assumed by the design formulas. On the contrary, its ability to relieve stress by creep or plastic flow, for example, partly compensates for its inherently low tensile strength and for uncertainties arising from redundancy. To be remembered also is the fact that, in spite of the deficiencies of design-formulas, concrete structures on the whole perform their intended function. Nevertheless, it should be evident that concrete cannot be used as intelligently as it might be and cannot be studied effectively without a better knowledge as to the magnitude and distribution of stresses within it.

The purpose of this paper may be stated as follows:

First, to derive—on the basis of simplifying assumptions in regard to the properties of concrete—expressions for: (a) deformations of, and (b)

the distribution of shrinkage stresses in, concrete beams and slabs during the course of drying.

Second, to show by means of data from specimens under controlled conditions the manner and degree to which the equations apply to concrete.

Third, to suggest methods for studying some of the more fundamental properties of drying concrete.

No attempt will be made here to give a complete analysis of stresses in concrete. In particular, the effect of aggregate particles on the stresses within the hardened paste will not be considered.

Before expressions for shrinkage stresses in concrete can be derived, assumptions must be made in regard to the relation between shrinkage and moisture content and the laws controlling the flow of moisture in concrete as well as the relation between stress and strain.

The actual relationships are not as simple as could be desired. If the flow of water were entirely by vapor diffusion, if the vapor pressure of the water in the concrete were proportional to the moisture-content, and if permeability were independent of the moisture-content, then the differential equation for the flow of water would be a partial-differential equation known in physics and mathematics either as the *diffusion equation* or as the *equation of heat conduction*. Carlson,[1]* in a study of distribution of moisture in concrete, assumed that this equation applies. If the flow of water could be expressed by the diffusion equation and if the shrinkage (or swelling) tendency† of each elemental volume were linearly related to the moisture-content, the unrestrained shrinkage (or swelling) could also be expressed by the diffusion equation. This possibility was also considered by Carlson.[1] But the flow of water is different from that indicated by the diffusion equation, and the relationship between the change in moisture-content and unrestrained shrinkage is not linear as required by these equations. Moreover, satisfactory expressions for either the flow of water or the moisture-shrinkage relation have not been found.

It is believed that moisture in concrete flows partly as liquid in capillaries, partly as vapor, and partly as adsorbed liquid on the surface of the colloidal products of hydration. While drying progresses, the vapor pressure of the water remaining in the region losing water decreases progressively with the moisture content. This change in vapor pressure with change in moisture content is not linear with respect to moisture

*See references at end of text of Part 1.

†By shrinkage (or swelling) tendency is meant the unit linear deformation due to any cause other than stress that would occur in an infinitesimal element if the element were unrestrained by neighboring elements. It is not to be confused with the *average* unit deformation, commonly called shrinkage, of a so-called unrestrained specimen, nor with the resultant linear unit deformation which for the x-direction will be designated e_x. Hereinafter, the linear unit shrinkage tendency will be referred to either as unrestrained shrinkage, for clarity, or merely as shrinkage, for brevity.

content. Neither is the rate of flow proportional to the gradient in vapor pressure. The shapes and relative proportions of the spaces occupied by liquid and by vapor change as drying proceeds. This fact, as well as the non-uniformity of the spaces, is believed to be partly responsible for the way in which vapor pressure depends on moisture content and the way in which rate of flow depends on gradient of vapor pressure.

The volume-change-vs.-weight-loss relation is different for different concretes depending on the composition of the concrete and the conditions of curing. For the same concrete it is different during first shrinkage from what it is during the second or subsequent volume changes. If a saturated prism of concrete is allowed to dry, the ratio of change of length to loss of water increases as drying proceeds. At first, comparatively small changes of volume occur per unit loss of weight. The higher the water-cement ratio and the shorter the period of curing the smaller the change during the initial stages of drying. Later the ratio becomes much larger and remains almost constant for some time, after which it may either increase or decrease as the specimen approaches its final weight. It is believed that this ratio, at any stage of drying, depends upon (a) the shape, size, and degree of uniformity of the spaces that hold the water; (b) the shape, size, rigidity, and spacing of the solid particles; and (c) the strength of the bonds between particles.

The relations between stress and strain must be considered in any study of volume changes resulting from moisture changes in concrete because any tendency for a change in volume that progresses from the surface inward always develops stresses. The stresses in turn, through the stress-strain relation, modify the resultant deformations. For low stresses both the elastic and inelastic strain produced by stress are approximately proportional to the stress, permitting Hooke's law to be assumed, but under most conditions of drying the shrinkage stresses, either alone or in combination with stresses from other sources, may be large enough to cause cracks and structural damage within the concrete and for such stresses the proportionality does not hold. Moreover, the apparent plasticity of an element* is greater during the time the element is drying for the first time than at any other time. The relative positions of the colloidal gel particles are no doubt changed by drying and while the changes are taking place small resultant stresses on an element will produce relatively large inelastic deformations.

In spite of the apparent difficulties of obtaining a satisfactory solution to the problem of deformations and stresses in concrete exposed to changes in ambient conditions, a relatively simple procedure has proved to be rather successful. The procedure is to assume as Carlson did that

*The reference is to an element of hydrated paste of just sufficient size to be a representative sample of the paste.

the diffusion equation applies to shrinkage even though the simple relations that are implied by that assumption are contrary to fact. It is further assumed that concrete follows Hooke's law. The derivations given in Part 1 are based upon these assumptions.

Since in Part 1 the derivations for deformations and stresses are based on the assumptions that shrinkage follows the diffusion equation and the material follows Hooke's law, the equations are even more applicable to thermal stresses in metals than to shrinkage stresses in concrete. In fact, much of the mathematical work given here was taken from the literature on diffusion of heat and on thermal stresses, as the references will show. However, certain corresponding coefficients in the two problems are of an entirely different order of magnitude. For example, the numerical value of the thermal diffusivity for steel expressed in square inches *per second* is approximately the same as the numerical value of the shrinkage diffusivity of concrete expressed in square inches *per day*. Because of the relatively slow diffusion of shrinkage the application of the hypothesis to the shrinkage of concrete necessitates the study of early transient conditions (usually ignored in the treatment of heat).

PART 1—SHRINKING (OR SWELLING), ITS EFFECT UPON DISPLACEMENTS AND STRESSES IN SLABS AND BEAMS OF HOMOGENEOUS, ISOTROPIC, ELASTIC MATERIAL

Notation

S = free, unrestrained unit linear shrinkage-strain
$-S$ = free, unrestrained unit linear swelling-strain
S_∞ = final shrinkage-strain under fixed ambient conditions, value of S when $t = \infty$
S_{av} = average shrinkage over the volume of the specimen, the same as average shortening per unit length if the material follows Hooke's law
t = time in days
k = diffusivity coefficient of shrinkage in sq. in. per day
f = surface factor, characteristic of the material and the boundary conditions, in in. per day
a, b, c, d, l = distances related to the dimensions of the specimen in inches
$B = fb/k$, a non-dimensional parameter
$T = kt/b^2$, a non-dimensional parameter
B_c and T_c, non-dimensional parameters corresponding to B and T and used when a second characteristic dimension of the specimen must be considered
x, y, z = rectangular coordinates
β_n = nth root of $\beta \tan \beta = B$
β_m = same as β_n except used in connection with c, whereas β_n is used in connection with b
A_n = Fourier coefficient

$$F_n = \frac{2B}{B^2 + B + \beta_n^2}, \quad F_m = \frac{2B_c}{B_c^2 + B_c + \beta_m^2}$$

$$H_n = \frac{B}{\beta_n^2} F_n, \qquad H_m = \frac{B_c}{\beta_m^2} F_m$$

$$G_n = \left(\frac{1}{\cos \beta_n} - \frac{B}{2} - 1\right) \frac{F_n}{\beta_n^2}$$

σ_x, σ_y, σ_z = normal components of stress parallel to $x-$, $y-$, and $z-$axes—positive if tensile, negative if compressive.
ϵ_x, ϵ_y, ϵ_z = elongations in $x-$, $y-$, and $z-$directions
τ_{xy}, τ_{xz}, τ_{yz} = shearing-stress components
γ_{xy}, γ_{xz}, γ_{yz} = shearing-strain components
E = Young's modulus in psi.
μ = Poisson's ratio
v = deflection in inches, displacement of the elastic line in the y-direction
N = the normal to the surface directed outward

$$P(x) = \frac{2}{\sqrt{\pi}} \int_0^x e^{-x^2} dx, \text{ the probability integral}$$

$$\phi(x) = \frac{2}{\sqrt{\pi}} \int_x^\infty e^{-x^2} dx = 1 - P(x)$$

$$\phi_b = 1 - \sum_1^\infty e^{-T\beta_n^2} F_n \frac{\cos \beta_n \frac{y}{b}}{\cos \beta_n}$$

$$\phi_c = 1 - \sum_1^\infty e^{-T_c\beta_m^2} F_m \frac{\cos \beta_m \frac{z}{c}}{\cos \beta_m}$$

$$H_b = 1 - \sum_1^\infty e^{-T\beta_n^2} H_n$$

$$H_c = 1 - \sum_1^\infty e^{-T_c\beta_m^2} H_m$$

Equation for diffusion of unrestrained shrinkage

The diffusion equation is a mathematical statement of the fact that for each infinitesimal volume of a body the excess of the substance in question flowing in over that flowing out per unit of time is equal to the rate of increase of the substance in that volume. When similar assumptions are made in regard to shrinkage, shrinkage thus being treated as if it were a "substance" just as heat is so treated, the result is[2]

$$k\left[\frac{\partial^2 S}{\partial x^2} + \frac{\partial^2 S}{\partial y^2} + \frac{\partial^2 S}{\partial z^2}\right] = \frac{\partial S}{\partial t} \quad \ldots\ldots\ldots\ldots\ldots\ldots\ldots\ldots (1)$$

where k is the diffusivity of shrinkage.

The equation becomes

$$k \frac{\partial S}{\partial N} = f(S_\infty - S) \quad \ldots\ldots\ldots\ldots\ldots\ldots\ldots\ldots\ldots\ldots\ldots\ldots (2)$$

at exposed boundaries and

$$\frac{\partial S}{\partial N} = 0 \qquad (3)$$

at sealed boundaries

where

N is the normal to the surface, directed away from the body

f is the surface factor

S_∞ is the value that S will eventually reach under fixed ambient conditions.

Equations 2 and 3 correspond, respectively, to Newton's law of cooling at exposed boundaries and to no flow of heat past perfectly insulated boundaries in the analogous problem of flow of heat.

If the boundaries of the body are not parallel planes, a transformation of Equation 1 from an expression in rectangular coordinates to some other form is usually desirable. For example, if the body is a circular cylinder, Equation 1 is best transformed to

$$k\left[\frac{\partial^2 S}{\partial r^2} + \frac{1}{r}\frac{\partial S}{\partial r} + \frac{1}{r^2}\frac{\partial^2 S}{\partial \Theta^2} + \frac{\partial^2 S}{\partial z^2}\right] = \frac{\partial S}{\partial t}$$

where r, Θ, and z are cylindrical coordinates. Frequently, the condition $\frac{\partial S}{\partial N} = 0$ at some boundaries or some other conditions will make S independent of certain coordinates and thereby simplify Equation 1.

Since the form of the solution for S depends upon the form of the differential equation, the form of the solution is dependent upon the boundary condition and the shape of the body under investigation. The initial conditions (values of S at $t = 0$) and any variation in boundary conditions with time will also affect the form of the solution.

Assumptions as to elastic properties

After a satisfactory solution for S has been obtained, then displacements and stresses will be found by the application of certain fundamentals of the theory of elasticity. The solutions for stresses are here restricted to homogeneous isotropic solids that follow Hooke's law. Also, as will be brought out below, the effect of Poisson's ratio will be neglected in some cases.

Effect of shape of body on relative values of principal stresses

The state of stress at any point in a body is defined by the directions and magnitudes of the three principal stresses. The three principal stresses in wide slabs and in narrow beams will be in the directions of length, width, and depth, respectively, if the bodies are under uniform exposure either from one or from two opposite faces and are without external restraint. The principal stress in the direction of depth (normal

to the exposed face) will be zero. The other two principal stresses will be equal in a wide slab (width large compared to depth) if the slab is either not restrained or is restrained equally in the directions of length and width; but in a narrow beam (width small compared to depth) the principal stress in the direction of width will be negligible, and the stress in the direction of length will be $(1 - \mu)$ times the corresponding stress in a corresponding slab. A corresponding slab differs from the beam just described primarily only in the matter of width. Beams whose widths are not small compared to their depths will have longitudinal stresses intermediate between those of slabs and narrow beams. Corresponding slabs and beams would, of course, have the same longitudinal stresses regardless of widths if Poisson's ratio were zero. Mathematical analyses will be made for the three cases shown in Fig. 1.*

To simplify the mathematical work the effects of Poisson's ratio will be neglected in most of the derivations for Cases I and II. When these effects are neglected, the results will be strictly correct only if Poisson's ratio is zero or if the beam is very narrow.

CASE I—SLAB OR BEAM DRYING FROM ONE FACE ONLY

Shrinkage

Solution by Fourier series. The exposed face of the slab or beam will be taken as the plane $y = h$, and the opposite face will be taken as the plane $y = 0$ as shown in Fig. 1 for Case I. For this case the diffusion equation reduces to

$$k \frac{\partial^2 S}{\partial y^2} = \frac{\partial S}{\partial t} \quad \ldots (1a)$$

The equation becomes

$$\frac{\partial S}{\partial y} = \frac{f}{k} (S_\infty - S) \quad \ldots (2a)$$

at the exposed boundary $y = h$ and

$$\frac{\partial S}{\partial y} = 0 \quad \ldots (3a)$$

at the sealed boundary $y = 0$.

A general solution for S satisfying Equations 1a and 3a is

$$S = S_\infty - \sum_1^\infty A_n e^{-\frac{kt}{h^2} \beta_n^2} \cos \beta_n \frac{y}{h} \quad \ldots (4)$$

*All figures and tables pertaining to Part I will be found on pages 196 to 204.

Equation 2a is also satisfied if β_n is the nth root of

$$\beta \tan \beta = \frac{fb}{k} \quad \ldots\ldots (2b)$$

i.e.,

$$\beta_n \tan \beta_n = \frac{fb}{k} \quad \ldots\ldots (2c)$$

The above statements may be verified by substituting S from Equation 4 into Equations 1a, 2a and 3a.

For time $t = \infty$, Equation 4 reduces to $S = S_\infty$, which is in accord with the definition of S_∞. An infinite series of terms such as the trigonometric series in Equation 4 is necessary to give an arbitrary distribution of shrinkage at time $t = 0$.

If the initial conditions are such that $S = 0$ when $t = 0$, then the Fourier coefficients A_n are given by*

$$A_n = \frac{S_\infty}{\cos \beta_n} \frac{2\frac{fb}{k}}{\left(\frac{fb}{k}\right)^2 + \frac{fb}{k} + \beta_n^2}$$

It therefore follows that

$$\frac{S}{S_\infty} = 1 - \sum_1^\infty e^{-T\beta_n^2} F_n \frac{\cos \beta_n \frac{y}{b}}{\cos \beta_n} \quad \ldots\ldots (5)$$

where

$$T = \frac{kt}{b^2}$$

$$F_n = \frac{2B}{B^2 + B + \beta_n^2}$$

$$B = \frac{fb}{k}$$

Equation 5 (in slightly different form) and similar equations for other shapes and other conditions, applied to analogous phenomena, may be found in the literature of mathematical physics such as the textbooks of Byerly, Carslaw, and Ingersoll and Zobel. Various tables and diagrams have been prepared from which the numerical relationship of the four non-dimensional quantities S/S_∞, y/b, B, and T may be found, such as Fig. 4, page 841 of Perry's *Chemical Engineer's Handbook* (1934).

*The general procedure of obtaining Fourier coefficients to satisfy initial conditions somewhat analogous to the present problem is given in Articles 66 to 68 of Byerly's *Fourier Series and Spherical Harmonics* Boston: Ginn & Co., 1893).

To use more than a few of the terms in Equation 5 for the evaluation of S/S_∞ is very laborious because of the difficulty in evaluating β_n and F_n. The number of terms required for a given degree of precision will depend somewhat upon the parameters B and y/b but is chiefly controlled by the parameter T. Computations show that very little error is introduced by neglecting all terms in the series except the first if T is more than about 0.2; but many terms are needed for the usually desired precision if T is less than 0.02,—the smaller the value of T the greater the number of terms needed. Very precise values of S/S_∞ for small values of T may be found without the tedious computation indicated in Equation 5 by using another expression which will now be derived.

Solution in terms of the probability integral. As long as the shrinkage at the sealed surface remains negligible, the distribution of shrinkage from the exposed surface inward will be nearly independent of the distance between the two surfaces. Suppose that instead of considering the surface at $y = 0$ to be sealed, the body is considered to be extended to infinity in a negative y-direction. Then instead of the boundary condition $\frac{\partial S}{\partial y} = 0$ at $y = 0$, the requirement will be

$$S = 0 \quad \text{.....(6)}$$

at $y = -\infty$.

The solution* satisfying Equations 1a, 2a and 6 and giving $S = 0$ when $t = 0$ is

$$\frac{S}{S_\infty} = \phi\left[\frac{1 - \frac{y}{b}}{2\sqrt{T}}\right] - \phi\left[\frac{1 - \frac{y}{b}}{2\sqrt{T}}\right] e^{B\left(1 - \frac{y}{b}\right) + B^2 T} \quad \text{.....(7)}$$

where $\phi(x)$ is $\frac{2}{\sqrt{\pi}} \int_x^\infty e^{-x^2}\, dx$ and T is again used in place of $\frac{kt}{b^2}$.

The quantity $1 - \phi(x)$, or $\frac{2}{\sqrt{\pi}} \int_0^x e^{-x^2}\, dx$, is known as the probability integral. Values of $\phi(x)$ may be readily found by using a table of the probability integral.

Numerical calculations show that Equation 7 gives values that differ from those given by Equation 5 by an amount less than the value of S/S_∞ at $y = 0$; therefore, Equation 7 may be used in place of Equation 5 whenever T is so small that S/S_∞ at $y = 0$ is less than the permissible error.

*This solution is very similar to that given for an analogous problem by Carslaw in Article 25 of *The Conduction of Heat*, (Macmillan & Co., Ltd., 2d ed., 1921).

Table 2 and Fig. 7, showing S/S_∞ in terms of y/b, kt/b^2, and fb/k, were prepared from Equations 5 and 7.

Stresses and strains

Continuity, Hooke's law and equilibrium. As stated previously, the solutions for stresses are here restricted to homogeneous, isotropic solids that follow Hooke's law. Equations for the stresses that would be produced in such a body by the shrinkages given by Equations 5 or 7 will now be derived.

The shrinkage S has been defined as the linear unit deformation that would occur if each infinitesimal element were unrestrained. However, the properties of a continuous solid will not permit an arbitrary distribution of deformations; therefore, unless the distribution of shrinkage given by Equation 5 happens to be compatible with the conditions of continuity, stresses will be produced that will modify the deformations so as to make them compatible. Although in general six partial differential equations are required for a complete mathematical statement of the conditions of compatibility,[3] these are reduced to

$$\frac{\partial^2 e_x}{\partial y^2} = 0 \qquad (8)$$

for either long narrow beams (plane stress) or slabs (plane strain) if the stresses are considered to be independent of the longitudinal coordinate x.

The term e_x is defined as the resultant unit deformation in the x-direction (the direction of length). It is therefore the algebraic sum of shrinkage, S, and the strain produced by stresses. σ_y is obviously zero; and if Poisson's ratio is zero or if the discussion is confined to narrow beams, σ_z is negligible. Therefore,

$$e_x = \frac{\sigma_x}{E} - S \qquad (9)$$

or, solving for stress,

$$\sigma_x = E\,(e_x + S) \qquad (10)$$

where E is Young's modulus.

The restriction imposed by Equation 8 requiring that the expression for longitudinal deformation contain no terms in y other than the first power (second derivative equal to zero) is equivalent to the assumption usually made in the elementary theory of beams that "plane cross-sections remain plane." If longitudinal restraint is complete, then e_x is zero and it follows from Equation 10 that $\sigma_x = ES$. If, however, longitudinal shortening is permitted but complete restraint against bending is provided, then e_x is not zero but is still independent of y. If the beam has no external restraint, the non-symmetrical distribution of shrinkage causes it to warp, making e_x a linear function of y. For no external restraint the equations of

equilibrium (summation of forces in the x-direction equal to zero and summation of moments about the z-axis equal to zero) become

$$\int_0^b \sigma_z \, dy = 0 \quad \ldots\ldots (11)$$

and

$$\int_0^b \sigma_z y \, dy = 0 \quad \ldots\ldots (12)$$

It may be shown by substituting Equation 10 into both Equations 11 and 12 that if shrinkage (S) is either independent of or a linear function of y, an unrestrained beam will be free of stress ($e_z = -S$ and $\sigma_z = 0$). For any other variation of shrinkage a stressed condition must result because the restriction on e_z (Equation 8) will not permit it to be equal and opposite to S if shrinkage is a non-linear function of y.

The only solution for e_z that satisfies Equations 8, 10, 11 and 12 is

$$e_z = \left(6\frac{y}{b} - 4\right)\frac{1}{b}\int_0^b S \, dy + \left(6 - 12\frac{y}{b}\right)\frac{1}{b^2}\int_0^b Sy \, dy. \quad (13)$$

When this value of e_z is substituted into Equation 10, the result is

$$\sigma_z = E\left[S + \left(6\frac{y}{b} - 4\right)\frac{1}{b}\int_0^b S \, dy + \left(6 - 12\frac{y}{b}\right)\frac{1}{b^2}\int_0^b Sy \, dy\right] \quad (14)$$

Finally, S from Equation 5 may be substituted into Equation 14, thus giving stress in an unrestrained beam as a function of the parameters y/b, kt/b^2, fb/k, S_∞ and of Young's modulus. This substitution will not be made until later, because it seems advisable at this time to consider another approach.

Solution by superposition. Although the above derivation is short and is in the simplest form for checking the mathematical correctness of the equation, a derivation in which elementary solutions are superposed is also desirable because it will be easier in general to understand and because the final expressions are in more usable forms. In this second derivation the resultant stress σ_z is considered as consisting of three parts. The first part is that stress which would be produced by complete restraint against longitudinal deformation; the second part is a uniform stress equal to and opposite in sign to the average of the first part; the third part is a stress

resulting from a simple moment that is equal to and opposite in sign to the moment produced by the sum of the first two parts. That is, the first part alone σ_x' would result from complete restraint, the sum of the first and second parts σ_x'' would result from restraint against warping only; the sum of all three parts, i.e., σ_x, would result if no external restraint were applied during shrinkage.

Although in this derivation an expression for σ_x appears to be the ultimate goal, expressions for σ_x' and for σ_x'' are also desirable. The stress σ_x' may be representative of the stress in pavement slabs or building walls that are restrained from shortening and the stress σ_x'' is representative of an unrestrained wall drying equally from two opposite sides (Case II discussed later).

Since for complete longitudinal restraint $e_x = 0$, it follows from Equation 10 that the first part of the stress is

$$\sigma_x' = ES \qquad (15)$$

Since the average value of σ_x' is $\frac{1}{b}\int_0^b \sigma_x'\, dy$, the second part of σ_x is $-\frac{E}{b}\int_0^b S\, dy$; therefore, the sum of the first and second parts (σ_x'') is given by

$$\sigma_x'' = E\left[S - \frac{1}{b}\int_0^b S\, dy\right] \qquad (16)$$

The moment produced by σ_x'' is the moment necessary to prevent warping. This moment per unit width of beam is found by multiplying Equation 16 by $y\, dy$ and integrating. This gives

$$M = \int_0^b \sigma_x''\, y\, dy = E\left[\int_0^b Sy\, dy - \frac{b}{2}\int_0^b S\, dy\right] \qquad (17)$$

For no external restraint this moment must be removed by superposing an equal and opposite moment. The stress resulting from a moment $-M$ is given by the elementary theory of beams as

$$\frac{M\,(y - b/2)}{1/12\; b^3}$$

This becomes

$$E\left(6 - 12\frac{y}{b}\right)\left[\frac{1}{b^3}\int_0^b Sy\,dy - \frac{1}{2b}\int_0^b S\,dy\right]$$

when M from Equation 17 is substituted. When this stress, the third part of σ_x is added to the sum of the first and second parts of Equation 16, the result is Equation 14 previously derived.

Stresses in terms of shortening and warping. The shortening of the beam can be considered as due to the second part of the stress since it is the addition of this part that removes longitudinal restraint and thereby permits the shortening of the beam. From these considerations it follows that

$$\text{unit shortening} = S_m = \frac{1}{b}\int_0^b S\,dy \qquad (18)$$

where S_m is the average value of S.

The bending (warping) of the beam can be considered as due to the third part of the stress since it is the addition of this part that removes the remaining external restraint and thereby permits warping of the beam. The deflection v caused by the moment $-M$ is given by the elementary theory of the bending of beams as $v = \frac{6Mx\,(l - x)}{Eb^3}$ where l is the span and v is the deflection of points within the span with respect to either of the end points $x = 0$ and $x = l$. The maximum deflection v_{max} (warping) that occurs at $x = l/2$ is therefore

$$v_{max} = \frac{6M}{Eb^3}\left(\frac{l}{2}\right)^2 = \frac{3l^2}{2b}\left[\frac{1}{b^3}\int_0^b Sy\,dy - \frac{1}{2b}\int_0^b S\,dy\right]^* \qquad (19)$$

By writing the second part of σ_x, $-\frac{E}{b}\int_0^b S\,dy$, in terms of the unit shortening S_m it produces, and by writing the third part of σ_x

$$E\left(6 - 12\frac{y}{b}\right)\left[\frac{1}{b^3}\int_0^b S\,y\,dy - \frac{1}{2b}\int_0^b S\,dy\right],$$

*The part in the brackets is numerically equal to one-sixth of the unit stress s that would be produced in either the top or the bottom of the beam by a moment just sufficient to straighten it. That is,

$$\frac{1}{6}s = \frac{M_{straight}}{Sb^2}$$

in terms of the deflection v_{max} it produces, the expressions for the stresses are put into more usable forms. When this is done, the following equations for stresses are obtained.

For complete longitudinal restraint (first part of σ_x),

$$\sigma_x' = ES \quad \ldots\ldots (15)$$

For restraint against warping only (sum of first and second parts of σ_x),

$$\sigma_x'' = E\,(S - S_{av}) \quad \ldots\ldots (20)$$

For no external restraint (sum of all three parts of σ_x),

$$\sigma_x = E\left[S - S_{av} + \left(6 - 12\frac{y}{b}\right)\frac{2bv_{max}}{3l^2}\right] \quad \ldots\ldots (21)$$

Evaluation of the parameters $\dfrac{S_{av}}{S_\infty}$ *and* $\dfrac{2bv_{max}}{3l^2S_\infty}$. When Equation 5 for S/S_∞ is substituted in Equation 18 for shortening and in Equation 19 for warping and the indicated integrations are performed, the result is

$$\frac{S_{av}}{S_\infty} = \frac{1}{b}\int_0^b \frac{S}{S_\infty}\,dy = 1 - \sum_1^\infty e^{-T\beta_n^2} H_n \quad \ldots\ldots (22)$$

$$\frac{2bv_{max}}{3l^2S_\infty} = \frac{1}{b^2}\int_0^b \frac{S}{S_\infty}\,y\,dy - \frac{S_{av}}{2S_\infty} = \sum_1^\infty e^{-T\beta_n^2} G_n \quad \ldots\ldots (23)$$

where

$$H_n = \frac{2B^2}{\beta_n^2\,(B^2 + B + \beta_n^2)}$$

and

$$G_n = \left(\frac{1}{\cos\beta_n} - \frac{B}{2} - 1\right)\frac{F_n}{\beta_n^2}$$

If T, the non-dimensional time-factor, is small, the series in Equations 22 and 23 converge rather slowly, and in that case it is convenient to use the following equations obtained by substituting Equation 7 into Equations 18 and 19, respectively.*

$$\frac{S_{av}}{S_\infty} = \frac{1}{B}\left[e^{B^2T}\,\phi(B\sqrt{T}) - 1 + \frac{2B\sqrt{T}}{\sqrt{\pi}}\right] \quad \ldots\ldots (24)$$

*The lower integration limit for each integral is decreased from 0 to $-\infty$;

$$\frac{2bv_{max}}{3l^2S_\infty} = \left\{\left[\frac{1}{2B} + \frac{1}{B^2}\right]\left[e^{B^2T}\ \phi(B\sqrt{T}) - 1 + \frac{2B\sqrt{T}}{\sqrt{\pi}}\right] - T\right\} \quad \ldots (25)$$

Furthermore, if the parameter $B\sqrt{T}$ is very small, it is still better to use the following equations obtained by expanding the expressions in the brackets of Equations 24 and 25.

$$\frac{S_{av}}{S_\infty} = BT\left[1 - \frac{4}{3\sqrt{\pi}}B\sqrt{T} + \frac{1}{2}(B\sqrt{T})^2 - \frac{8}{15\sqrt{\pi}}(B\sqrt{T})^3 + \ldots\right] \quad (24a)$$

$$\frac{2bv_{max}}{3l^2S_\infty} = \left[\frac{BT}{2} - T\left(1 + \frac{B}{2}\right)\left(\frac{4}{3\sqrt{\pi}}B\sqrt{T} - \frac{1}{2}(B\sqrt{T})^2 + \frac{8}{15\sqrt{\pi}}(B\sqrt{T})^3\right) - \ldots\right] \quad \ldots (25a)$$

In general the following rules will be found applicable for rapid evaluation of the parameters $\frac{S_{av}}{S_\infty}$ and $\frac{2bv_{max}}{3l^2S_\infty}$ to a fair degree of accuracy.

If T is more than about 0.05, use Equations 22 and 23.

If T is less than about 0.05 and B is more than about 5, use Equations 24 and 25.

If T is less than about 0.05 and B is less than about 5, use Equations 24a and 25a.

Forces and moments necessary for complete restraint. The force necessary for longitudinal restraint is $\int \sigma_x' \, dA$. Therefore, the average force per unit area is $\frac{1}{b}\int_0^b \sigma_x' \, dy$. From Equations 15, 5, and 22 this becomes

$$\text{force per unit area} = ES_\infty\left[1 - \sum_1^\infty e^{-T\beta_n^2} H_n\right] \quad \ldots (26)$$

From Equations 17, 5, and 23, the moment per unit width necessary for restraint against warping is found to be

$$M = ES_\infty b^2 \sum_1^\infty e^{-T\beta_n^2} G_n \quad (27)$$

Simplification by taking B as equal to infinity. The principal equations derived above reduce to simpler forms and the computation of numerical values is less tedious if the assumption is made that B, i.e., fb/k, equals infinity. If B is large, say 100 or more, the error introduced by assuming it to be infinity is negligible. However, if B is less than about 5, the error introduced by considering it to be infinity may be appreciable as is shown, for example, by Fig. 8, 9, and 14. Whether justifiable or not, the assumption that $B = \infty$ is frequently made in analogous problems to which the diffusion equation applies. This assumption was made by Terzaghi and Fröhlich[4] in developing the theory of settlement of foundations due to consolidation of underlying material, by Glover[5] in a study of distribution of temperature in concrete dams, and by Carlson[1] in a study of distribution of moisture and shrinkage in concrete. The more important of the above equations for the special case of $B = \infty$ are given below:

Equation 5 becomes

$$\frac{S}{S_\infty} = 1 - \sum_1^\infty \frac{4\,(-1)^{n-1}}{(2n-1)\pi}\, e^{-(2n-1)^2 \frac{\pi^2}{4} T} \cos\,(2n-1)\frac{\pi y}{2b}.$$

Equation 7 becomes

$$\frac{S}{S_\infty} = \phi\left(\frac{1 - y/b}{2\sqrt{T}}\right).$$

Equation 22 becomes

$$\frac{S_{av}}{S_\infty} = 1 - \frac{8}{\pi^2} \sum_1^\infty \frac{1}{(2n-1)^2}\, e^{-(2n-1)^2\,(\pi^2/4)\,T}$$

Equation 24 becomes

$$\frac{S_{av}}{S_\infty} = \frac{2}{\sqrt{\pi}} \sqrt{T}.$$

Equation 23 becomes

$$\frac{2bv_{max}}{3l^2 S_\infty} = \sum_1^\infty \frac{4}{\pi^2\,(2n-1)^2}\left[\frac{(-1)^{n-1}\,4}{\pi\,(2n-1)} - 1\right] e^{-(2n-1)^2 \frac{\pi^2}{4} T}.$$

Equation 25 becomes

$$\frac{2bv_{max}}{3l^2 S_\infty} = \frac{\sqrt{T}}{\sqrt{\pi}} - T.$$

*Tables, curves, and computations.** Tables and diagrams such as those by Newman[6] are available from which values of S/S_∞ and S_{av}/S_∞ may be determined. However, such published tables are in general not adequate for the present problem. The smallest value of the parameter T used by Newman in his computations was 0.1, whereas the stresses in concrete may be desired for a much earlier period. The tables given here were prepared for T as low as 0.001. Moreover, so far as is known, the parameter $\frac{2bv_{max}}{3l^2S_\infty}$ had not previously been evaluated for this or any analogous problem and its evaluation is necessary for the problem here considered.

A step in the evaluation of Equations 15, 20, and 21 for the theoretical stresses in a beam drying from one side under the different modes of restraint is the evaluation of the three quantities $\frac{S}{S_\infty}$, $\frac{S_{av}}{S_\infty}$ and $\frac{2bv_{max}}{3l^2S_\infty}$. The first quantity S/S_∞ as a function of the three parameters y/b, B and T, is given in Table 2 and shown graphically in Fig. 7. The second quantity S_{av}/S_∞ as a function of B and T is given in Table 3 and shown graphically in Fig. 8.† The third quantity $\frac{2bv_{max}}{3l^2S_\infty}$ as a function of B and T is given in Table 4 and shown graphically in Fig. 9. Tables 5 and 6 giving the stresses σ_x'' and σ_x (Equations 20 and 21) as functions of the three parameters y/b, B, and T, were readily prepared after the three primary quantities had been evaluated (Tables 2, 3, and 4). Results for $B = 5$ are shown graphically in Fig. 10, 11, 12, and 13. Fig. 14 shows maximum values of $\frac{\sigma_x''}{ES_\infty}$ and $\frac{\sigma_x}{ES_\infty}$ and of $\frac{2bv_{max}}{3l^2S_\infty}$ versus the parameter B.

The computations made for the preparation of the tables and diagrams are explained in part below.

If the parameter T is so small that the equations based upon the assumption that the body extends to infinity may be used instead of the theoretically correct equations, no difficulty is encountered. For example, let $y/b = 0.8$, $B = 5$, and $T = 0.01$. Equation 7 then becomes

$$\frac{S}{S_\infty} = \phi\left(\frac{0.2}{2 \times 0.1}\right) - \phi\left(\frac{0.2}{2 \times 0.1} + 5 \times 0.1\right) e^{5 \times 0.2 + 25 \times 0.01}$$

$$= \phi(1) - \phi(1.5)\, e^{1.25}$$

*The values of β_n given in Table 1 differ slightly from those given by Newman in some instances. The values in Table 1 are believed to be accurate to the number of places given. The tables other than Table 1 have not been checked by duplicate computations. But, except for the last digit, which may be inaccurate by a point or two, these tables are believed to be reasonably accurate.

†In Fig. 8 and 9, where shortening and warping were the dependent variables, the square root of T for the abscissas was found to be better than T, because a considerable part of such graphs were approximately straight lines. For this reason the square root of T rather than T was used for the abscissas in the construction of these diagrams.

From mathematical tables

$$\phi\,(1) = 0.15730; \phi\,(1.5) = 0.03389; e^{1.25} = 3.4903$$

Therefore $S/S_\infty = 0.1573 - 0.03389 \times 3.4903 = 0.0390$.

Note that this is the value given in Table 2 for the above values of B, T, and y/b. Also note that for the same B and T the table gives zero for $y/b = 0$, showing that it was permissible to use Equation 7 instead of Equation 5.

When the theoretically correct equations are used, the computations are more involved. For instance, let $T = 0.1$ instead of 0.01 in the above example. T will then be so large that S/S_∞ will have an appreciable value at $y/b = 0$. Therefore, Equation 7 will not be applicable and Equation 5, the exact equation, must be used. A substitution of values for T and y/b into Equation 5 gives

$$\frac{S}{S_\infty} = 1 - \sum_{1}^{\infty} e^{-0.1\beta_n^2} F_n \frac{\cos 0.8\beta_n}{\cos \beta_n}$$

The first step in evaluating the above expression is to determine β_n which Equation 2c shows to be a function of fb/k and n, i.e., B, and the integer n. The determination of β_n by interpolation is simplified by the introduction of α_n where α_n depends on B and n. The equation for β_n is then written

$$\beta_n = (n - 1 + \alpha_n)\pi \quad \ldots\ldots\ldots\ldots\ldots\ldots\ldots\ldots\ldots\ldots (28)$$

Curves of α_n versus B for the first six values of n and for $n = 21$ are shown in Fig. 2. By means of Fig. 2 and Equation 28 any desired β_n may be found with reasonable accuracy for any value of B. The first six values of β_n for several different values of B are given in Table 1.

After finding β_n for the given values of B and n, the factors F_n, $\cos\beta_n$, $\cos\left(\beta_n \frac{y}{b}\right)$ and $e^{-T\beta_n^2}$ are determined. F_n and $\cos\beta_n$ as functions of B are shown in Fig. 3 and 4, respectively, for the first six values of n. The functions $\cos\left(\beta_n \frac{y}{b}\right)$ and $e^{-T\beta_n^2}$ are readily obtained from mathematical tables after the products $\beta_n \frac{y}{b}$ and $T\beta_n^2$ have been determined. When the proper values of the four factors listed above are substituted, the above equation for $\frac{S}{S_\infty}$ becomes

$$\frac{S}{S_\infty} = 1 - \frac{0.84147 \times 0.3152 \times 0.4966}{0.2541} - \frac{0.1965 \times 0.2161 \times 0.9963}{0.6277}$$
$$- \frac{0.00844 \times 0.1286 \times 0.7280}{0.8101} + \quad . \quad . \quad . \quad .$$

This reduces to $\frac{S}{S_\infty} = 1 - 0.5183 - 0.0674 - 0.0009 = 0.4134$

The values for S/S_∞ given in Table 2 were computed by one or the other of the methods illustrated above.

In preparing Table 3 from which Fig. 8 was constructed (Fig. 8 shows shortening as a function of $\sqrt{T}$ for various values of B), values of H_n in Equation 22 were needed. Values of H_n as a function of B for the first six values of n are shown in Fig. 5. In like manner, Fig. 6 showing G_n as a function of B, served in the preparation of Table 4 from which Fig. 9 was constructed. Of course, for small values of T, Fig. 5 and 6 are not necessary since either Equation 24 or Equation 24a is used instead of Equation 22 and either Equation 25 or Equation 25a is used instead of Equation 23, depending on the value of B.

Application to beams or slabs of any width-to-depth ratio when Poisson's ratio is not zero. The effect of Poisson's ratio was neglected in the preceding derivations. Its effect stated in general terms in the introductory remarks in regard to Case I will now be analyzed in more detail. If Poisson's ratio is not zero, Equation 9 for e_x and Equation 10 for σ_x will be modified to include the effect of σ_z. That is,

$$e_x = \frac{\sigma_x}{E} - \frac{\mu \sigma_z}{E} - S \quad \ldots\ldots\ldots\ldots\ldots\ldots\ldots\ldots\ldots\ldots \quad (9a)$$

$$\sigma_x - \mu\sigma_z = E\,(e_x + S) \quad \ldots\ldots\ldots\ldots\ldots\ldots\ldots\ldots\ldots\ldots \quad (10a)$$

However, if the ratio of width to depth is small, σ_z will be negligible and Equation 10a reduces to Equation 10. On the other hand, if the ratio of width to depth is very large (a slab), the width being comparable with the length, then σ_z will be equal to σ_x. If $\sigma_x = \sigma_z$, then Equation 10a reduces to

$$\sigma_x = \frac{E}{1 - \mu} \cdot (e_x + S) \quad \ldots\ldots\ldots\ldots\ldots\ldots\ldots\ldots\ldots\ldots \quad (10b)$$

The only difference between Equation 10b for a wide slab and Equation 10 for a narrow beam is the factor μ, which occurs in Equation 10b but not in Equation 10. Therefore, for stresses in a slab, E in Equations 15, 20, and 21 is replaced by $\frac{E}{1 - \mu}$. The stresses in beams whose width-to-depth ratio is intermediate will have stresses intermediate between those of narrow beams and of slabs. Since E does not appear in Equa-

tion 22 for average shrinkage nor in Equation 23 for warping, these quantities are the same for narrow beams and wide slabs.

CASE II—SLAB OR BEAM DRYING FROM TWO OPPOSITE SURFACES

Equations taken from those derived for Case I. Since the flow of moisture in a slab drying from only one surface is believed to be the same as that in either half of a slab of twice the depth drying from two opposite surfaces, it will be assumed that the theoretical equations derived for shrinkage of a beam or slab drying from only one surface will apply equally well for either half of a beam or slab drying from two opposite surfaces. The plane midway between the drying surfaces will be taken as the plane $y = 0$ as shown in Fig. 1 for Case II. Since the two halves of the beam will mutually restrain each other from warping, the equations for stresses, strains, and shortening in each half will be the same as those given previously in Case I for a beam restrained against warping and drying from one surface.

CASE III—RECTANGULAR PRISM DRYING FROM FOUR FACES

Shrinkage

The differential equation and boundary conditions. For a prism drying from four faces but not from the ends the diffusion equation reduces to

$$k\left(\frac{\partial^2 S}{\partial y^2} + \frac{\partial^2 S}{\partial z^2}\right) = \frac{\partial S}{\partial t} \qquad (1b)$$

The exposed faces of the prism will be taken as the planes $y = \pm b$, $z = \pm c$, as shown in Fig. 1 for Case III. The boundary conditions then become

$$\frac{\partial S}{\partial y} = \pm \frac{f}{k}(S_\infty - S) \qquad (2a)$$

at the boundaries $y = \pm b$ and

$$\frac{\partial S}{\partial z} = \pm \frac{f}{k}(S_\infty - S) \qquad (3b)$$

at the boundaries $z = \pm c$.

The solution satisfying Equations 1b, 2a, 3b, and giving $S = 0$ at $t = 0$ and $S = S_\infty$ at $t = \infty$ is the following:

$$\frac{S}{S_\infty} = 1 - \left[\sum_1^\infty e^{-T\beta_n^2} \frac{\cos \beta_n \frac{y}{b}}{F_n \cos \beta_n}\right]\left[\sum_1^\infty e^{-T_c \beta_m^2} \frac{\cos \beta_m \frac{z}{c}}{F_m \cos \beta_m}\right] \qquad (5a)$$

where β_m, F_m, and T_c correspond to β_n, F_n, and T, respectively, the difference being that the dimension b has been replaced by c.

Shrinkage expressed in terms of the solutions given for a prism drying from one face or two opposite faces. Since the infinite series in the first bracket in Equation 5a is identical with the one given in Equation 5 and the infinite series in the second bracket is like the first except that y is replaced by z, b by c, etc., and since Equation 5 applies to either half of a slab exposed on two opposite surfaces (Case II), it follows that the brackets have the following values:

$$\Sigma e^{-T\beta_n^2} F_n \frac{\cos \beta_n \frac{y}{b}}{\cos \beta_n} = 1 - \phi_b \quad \ldots\ldots (29)$$

$$\Sigma e^{-T_c\beta_m^2} F_m \frac{\cos \beta_m \frac{z}{c}}{\cos \beta_m} = 1 - \phi_c \quad \ldots\ldots (30)$$

where ϕ_b is the value S/S_∞ would have if only the surfaces $y = \pm b$ were exposed and ϕ_c is the value S/S_∞ would have if only the surfaces $z = \pm c$ were exposed.

A substitution of Equations 29 and 30 into Equation 5a gives

$$\frac{S}{S_\infty} = \phi_b + \phi_c - \phi_b\phi_c \quad \ldots\ldots (5b)$$

Equation 5b shows that the evaluation of shrinkage for a prism drying from four surfaces becomes a problem of adding the independent effects of drying from surfaces that are perpendicular to each other and then subtracting a term proportional to the product of the separate effects.

For example, consider the shrinkage tendency at the point $y = 0.4b$, $z = 0.8c$ in a prism for which $c = 2b$ (width equal to twice the thickness). Let f, k, and t be such that $fb/k = 5.0$ and $kt/b^2 = 0.20$; then $fc/k = 10.0$ and $kt/c^2 = 0.05$. ϕ_b is found in Table 2 or from Fig. 7 to be 0.2398. Since Table 2 was prepared for B equal to 0.1, 1.0, 5.0, and ∞ only, and since $fc/k = 10$, ϕ_c can be found from Table 2 only by interpolation. However, examination of Table 2 indicates that for kt/c^2 equal to 0.05 Equation 7 can be used instead of Equation 5 without appreciable error and therefore the equation rather than the table will be used to obtain ϕ_c. From Equation 7

$$\phi_c = \phi\left(\frac{0.2}{2\sqrt{0.05}}\right) - \phi\left(\frac{0.2}{2\sqrt{0.05}} + 10\sqrt{0.05}\right) e^{2+5}.$$

From tables giving probability integrals and the exponential function

$$\phi_c = 0.5273 - 0.000156 \times 1097 = 0.355.$$

Therefore at $y = 0.4b$, $z = 0.8c$, and $t = 0.20\ b^2/k$,

$$\frac{S}{S_\infty} = 0.2398 + 0.355 - 0.2398 \times 0.355 = 0.510.$$

Shortening expressed in terms of the shortening of a prism drying from one face or from two opposite faces. The average shrinkage S_{av} is given by

$$S_{av} = \frac{1}{bc} \int_0^b \int_0^c S \, dy \, dz \quad \text{(18a)}$$

From Equations 5a and 18a

$$\frac{S_{av}}{S_\infty} = 1 - \sum_1^\infty e^{-T\beta_n^2} H_n \sum_1^\infty e^{-T_c \beta_m^2} H_m \quad \text{(22a)}$$

or

$$\frac{S_{av}}{S_\infty} = H_b + H_c - H_b H_c, \quad \text{(22b)}$$

where H_b is the value S_{av}/S_∞ would have if only the surface $y = \pm b$ were exposed and H_c is the value S_{av}/S_∞ would have if only the surfaces $z = \pm c$ were exposed*. Therefore, the average shrinkage, and consequently the shortening, if the body is elastic, of a prism drying from four sides may be found by considering the separate effects of drying from opposite sides in pairs.

For example, consider the shortening of the prism discussed above. H_b is found in Table 3 to be 0.3510 and H_c is found to be 0.1753. Therefore,

$$\frac{S_{av}}{S_\infty} = 0.3510 + 0.1753 - 0.3510 \times 0.1753 = 0.4647.$$

Stresses and strains

Nature of the problem and the method to be used to obtain a solution. In Cases I and II previously discussed, where shrinkage was a function of time t and only one space coordinate y and where the problem was further simplified by neglecting the effects of the length and the width of the specimen on the distribution of stresses, a solution for the one stress involved was readily obtained. However, in the problem now under consideration, a prism drying from four surfaces, shrinkage varies with an additional coordinate z. As a result stresses vary with this additional coordinate also, and more than one stress will be involved. The problem will be somewhat simplified by neglecting the effect of the length on the distribution of stresses, i.e., the assumption will be made that stresses do not vary along the length. The distribution of stresses given by the solution based on this assumption will deviate a negligible amount from

*If a prism were drying from all six surfaces, the corresponding equation would be $S_{av}/S_\infty = H_a + H_b + H_c - H_a H_b - H_b H_c - H_c H_a + H_a H_b H_c$. Another way of expressing these relations is given by Glover (Ref. 7).

the theoretically correct distribution when stresses in the central portion of a long prism are under consideration (principle of Saint Venant[8]).

The solution for shrinkage in terms of two space coordinates was almost as simple as when only one coordinate was involved (Equation 5a for Case III compared with Equation 5 for Cases I and II), because tendency to shrink is considered to be a scalar quantity. On the other hand, since stresses are tensor quantities, the solution for stresses usually becomes much more complicated whenever more than one coordinate is involved. In fact, elasticians have obtained exact solutions meeting all boundary conditions for only a relatively few problems in which stresses were functions of at least two coordinates and then only by considering the body to be infinite in the direction of one of these coordinates. The difficulty is that since stresses are tensors, boundary forces are vectors, and in two-dimensional problems two components of force must be satisfied at each boundary. The specified conditions of stress at any two opposite boundaries can be satisfied by superposing particular solutions of the differential equations in accordance with the usual methods of Fourier analysis. But, in general, solutions satisfying rigorously the boundary requirements at two pairs of opposite boundaries simultaneously cannot be found by the usual methods.

A method of solving such problems after the appropriate differential equations have been derived was explained by the author in a recent paper[9]. That method will be used here. It is about the same as that used previously by Taylor[10] and by Timoshenko[11] in analogous problems.

Derivation of the differential equations relating stresses to shrinkage. By neglecting the variation of stresses and strains along the length of a body the problem becomes a two-dimensional problem in plane strain. The following equations taken from the theory of elasticity are then applicable[12].

Equations of Equilibrium:

$$\frac{\partial \sigma_y}{\partial y} + \frac{\partial \tau_{yz}}{\partial z} = 0$$

$$\frac{\partial \sigma_z}{\partial z} + \frac{\partial \tau_{yz}}{\partial y} = 0$$

Condition of Compatibility:

$$\frac{\partial^2 e_y}{\partial z^2} + \frac{\partial^2 e_z}{\partial y^2} = \frac{\partial^2 \tau_{yz}}{\partial y \partial z}$$

Hooke's Law Modified to Include Isotropic Shrinkage:

$$e_z = \frac{1}{E}\left[\sigma_y - \mu\sigma_y - \mu\sigma_z\right] - S = -S_{ss} \text{ in this problem}$$

$$e_y = \frac{1}{E}[-\mu\sigma_x + \sigma_y - \mu\sigma_z] - S$$

$$e_z = \frac{1}{E}[-\mu\sigma_x - \mu\sigma_y + \sigma_z] - S$$

$$\gamma_{yz} = \frac{2(1+\mu)}{E}\tau_{yz}$$

The above seven equations giving relations between the eight unknown stresses and strains can be reduced to the following two equations by eliminating the four strains and the shear stress:

$$\sigma_x = \mu(\sigma_y + \sigma_z) + E(S - S_{av}) \quad \ldots\ldots (31)$$

$$\nabla^2(\sigma_y + \sigma_z) = \frac{E}{1-\mu}\nabla^2 S \quad \ldots\ldots (32)$$

where ∇^2 is written for $\frac{\partial^2}{\partial y^2} + \frac{\partial^2}{\partial y^2}$.

These two equations together with the two equations of equilibrium and the boundary conditions that

$$\sigma_y \text{ and } \tau_{yz} = 0 \text{ at } y = \pm b$$

$$\sigma_z \text{ and } \tau_{yz} = 0 \text{ at } z = \pm c$$

and Equation 5a for S constitute the mathematical statement of the problem.

Solution for stresses. In general the stress σ_x will be larger than either σ_y or σ_z. The stress τ_{yz} will be relatively small in all cases. If only the value of the theoretical maximum stress is desired, a fairly good approximation can be obtained by the following simplified formula:

$$\sigma_x = E(S - S_{av}) \text{ approx.} \quad \ldots\ldots (31a)$$

where S is given by Equation 5a and S_{av} is given by Equation 22a. If, however, an accurate theoretical value of all stresses is desired, a complete solution must be obtained and this is given below:

The solution for σ_y, σ_z, and τ_{yz} meeting all of the above requirements is as follows:*

$$\sigma_y = A_o\frac{c^2 - 3z^2}{12bc} + \frac{b}{c}\sum_{i=1}^{\infty}\sum_{j=1}^{\infty}\frac{A_{ij}}{i^2}\cos\alpha_i y\cos\gamma_j z$$

*Equations 33, 34, and 35 for stresses and Equations 36 and 37 for the coefficients B_j and C_i given here are almost the same as Equations 1, 2, and 3 for stresses and Equations 6 and 7 for the coefficients B_n and A_n respectively given in Ref. 9. The A_{ij}-series and the A_o-terms enter into the equations given here in place of the terms in the stress S given there; otherwise, except for slight differences in notation, the corresponding equations are identical and the equations given here may be derived by the procedures given there.

Equation 38 for A_{ij} and Equation 39 for A_o may be verified by substituting Equations 33, 34, and 5a into Equation 32 and then proving the equality of the two sides of the resulting equation within the domain under consideration by the usual Fourier analysis.

$$+ \sum_{j=1}^{\infty} B_j \frac{\cos \gamma_j z}{\cosh \gamma_j b} [\gamma_j y \sinh \gamma_j y - (1 + \gamma_j b \coth \gamma_j b) \cosh \gamma_j y]$$

$$- \sum_{i=1}^{\infty} C_i \frac{\cos \alpha_i y}{\cosh \alpha_i c} [\alpha_i z \sinh \alpha_i z + (1 - \alpha_i c \coth \alpha_i c) \cosh \alpha_i z] \quad (33)$$

$$\sigma_z = A_o \frac{b^2 - 3y^2}{12bc} + \frac{c}{b} \sum_{i=1}^{\infty} \sum_{j=1}^{\infty} \frac{A_{ij}}{j^2} \cos \alpha_i y \cos \gamma_j z$$

$$- \sum_{j=1}^{\infty} B_j \frac{\cos \gamma_j z}{\cosh \gamma_j b} [\gamma_j y \sinh \gamma_j y + (1 - \gamma_j b \coth \gamma_j b) \cosh \gamma_j y]$$

$$+ \sum_{i=1}^{\infty} C_i \frac{\cos \alpha_i y}{\cosh \alpha_i c} [\alpha_i z \sinh \alpha_i z - (1 + \alpha_i c \coth \alpha_i c) \cosh \alpha_i z] \quad (34)$$

$$\tau_{yz} = \sum_{i=1}^{\infty} \sum_{j=1}^{\infty} \frac{A_{ij}}{ij} \sin \alpha_i y \sin \gamma_j z$$

$$+ \sum_{j=1}^{\infty} B_j \frac{\sin \gamma_j z}{\cosh \gamma_j b} [\gamma_j b \coth \gamma_j b \sinh \gamma_j y - \gamma_j y \cosh \gamma_j y]$$

$$+ \sum_{i=1}^{\infty} C_i \frac{\sin \alpha_i y}{\cosh \alpha_i c} [\alpha_i c \coth \alpha_i c \sinh \alpha_i z - \alpha_i z \cosh \alpha_i z] \quad \ldots\ldots (35)$$

where $\alpha_i = \dfrac{i\pi}{b}$, $\gamma_j = \dfrac{j\pi}{c}$

$$B_j = \frac{- \dfrac{c}{b} \dfrac{A_o (-1)^j}{\pi^2 j^2} + \dfrac{b}{c} \displaystyle\sum_{i=1}^{\infty} (-1)^i \frac{A_{ij}}{i^2} - \sum_{i=1}^{\infty} (-1)^{i+j} \frac{4}{j\pi} \frac{ic}{jb} \dfrac{\tanh \dfrac{i\pi c}{b}}{\left[1 + \left(\dfrac{ic}{jb}\right)^2\right]^2} C_i}{1 + \dfrac{j\pi b}{c} \left(\coth \dfrac{j\pi b}{c} - \tanh \dfrac{j\pi b}{c}\right)}$$

$\ldots\ldots (36)$

$$C_i = \frac{-\frac{c}{b}\frac{A_o(-1)^i}{\pi^2 i^2} + \frac{c}{b}\sum_{j=1}^{\infty}(-1)^j\frac{A_{ij}}{j^2} - \sum_{j=1}^{\infty}(-1)^{i+j}\frac{4}{i\pi}\frac{jb}{ic}\frac{\tanh\frac{j\pi b}{c}}{\left[1+\left(\frac{jb}{ic}\right)^2\right]^2}B_i}{1+\frac{i\pi c}{b}\left(\coth\frac{i\pi c}{b} - \tanh\frac{i\pi c}{b}\right)} \quad \ldots\ldots (37)$$

$$A_{ij} = -\left[\frac{ES_\infty\, 4\,(-1)^{i+j}\, i^2 j^2}{(1-\mu)\,\pi^2\left(i^2\frac{c}{b} + j^2\frac{b}{c}\right)^2}\right] \sum_{n=1}^{\infty}\sum_{m=1}^{\infty}\frac{\left(\beta_n^2\frac{c}{b} + \beta_m^2\frac{b}{c}\right)e^{-T\beta_n^2}\, e^{-T_c\beta_m^2}\, H_n H_m}{\left(1-\frac{i^2\pi^2}{\beta_n^2}\right)\left(1-\frac{j^2\pi^2}{\beta_m^2}\right)} \quad (38)$$

$$A_o = -\frac{ES_\infty}{1-\mu}\sum_{n=1}^{\infty}\sum_{m=1}^{\infty}\left(\beta_n^2\frac{c}{b} + \beta_m^2\frac{b}{c}\right)e^{-T\beta_n^2}\, e^{-T_c\beta_m^2}\, H_n H_m \quad (39)$$

The above equations, together with Equation 31 for σ_x, constitute a complete solution on the basis of the given assumptions.

In general, if both the parameters T and T_c are equal to or greater than 0.1, the series given above converge very rapidly so that only a few terms need be taken for a good approximation. The example given below will demonstrate the use of the above equations.

Example: *Stress at the middle of one side of a square prism for which B equals 5 and at a time for which T equals 0.1.* If only one term in each series is used, the following values are obtained: From Equations 38 and 39 and Table 1.

$$A_o = -\frac{ES_\infty}{1-\mu}\,(\beta_1^2 + \beta_1^2)\, e^{-0.1\,\beta_1^2}\, e^{-0.1\,\beta_1^2}\, H_1^2$$

$$A_o = -\frac{ES_\infty}{1-\mu}(1.3138^2 + 1.3138^2)\, 0.8415^2 \times 0.9130^2$$

$$A_o = -2.0377\,\frac{ES_\infty}{1-\mu}$$

$$A_{11} = -\frac{ES_\infty}{(1-\mu)\,\pi^2}\,\frac{(1.3138^2 + 1.3138^2)\, 0.8415^2 \times 0.9130^2}{\left(1-\frac{\pi^2}{1.3138^2}\right)^2}.$$

$$A_{11} = -0.0093 \frac{ES_\infty}{1-\mu}$$

When these values are substituted into Equation 36, the result is

$$B_1 = \frac{\left(-\frac{2.0376}{\pi^2} + 0.0093\right)\frac{ES_\infty}{1-\mu} - \frac{tanh\,\pi}{\pi} C_1}{1 + \pi\,(coth\,\pi - tanh\,\pi)}$$

or since $C_1 = B_1$ (square prism),

$$C_1 = B_1 = -0.1472 \frac{ES_\infty}{1-\mu}$$

When the above values and $z = c$, $y = 0$ are substituted into Equation 33, the result is

$$\sigma_y \Big|_{\substack{z=c \\ y=0}} = \left[\frac{2.0377}{6} + 0.0093 - 0.1472 \times 0.3583 + 0.1472 \times 0.9773\right]\frac{ES_\infty}{1-\mu}$$

$$\sigma_y \Big|_{\substack{z=c \\ y=0}} = \left[+0.3396 + 0.0093 - 0.0527 + 0.1439\right]\frac{ES_\infty}{1-\mu} = 0.4401\,\frac{ES_\infty}{1-\mu}$$

When the summation of each series is carried to two terms, the result is $0.4214\,\frac{ES_\infty}{1-\mu}$ and when the summation is carried to four terms in each series the result is $0.4221\,\frac{ES_\infty}{1-\mu}$ for this stress.

The above shows that the series converge very rapidly for this example.

The stresses σ_z and τ_{yz} are obviously zero at the point under consideration.

From Equations 31, 5b, and 22b, Tables 2 and 3, and the above result for σ_y,

$$\sigma_x \Big|_{\substack{z=c \\ y=0}} = \left[\frac{\mu}{1-\mu}0.4221 + (0.0221 + 0.6913 - 0.0221 \times 0.6913) - (0.2186 + 0.2186 - 0.2186 \times 0.2186)\right]ES_\infty$$

$$\sigma_x \Big|_{\substack{z=c \\ y=0}} = \left[\frac{\mu}{1-\mu}\,0.4221 + 0.3087\right]ES_\infty$$

For all values of Poisson's ratio μ less than 0.212, the above expressions will give larger values for σ_y than for σ_x. This fact is of interest because,

in the similar problem of a long cylinder drying or cooling from the curved surface the two corresponding stresses are equal regardless of Poisson's ratio[9].

OTHER METHODS

A paper of this kind would not be complete without calling attention to the possibilities of using a *difference equation* instead of Equation 1. The *difference equation* that would replace Equation 1 would be a statement of the relation between the values of S at the point (x, y, z) at the time t and what the values of S were at this point and at points distant $\pm\Delta x$, $\pm\Delta y$ and $\pm\Delta z$ in the x-, y-, and z-directions, Δt units of time previously. In the limit as Δx, Δy, Δz and Δt are made smaller, the *difference equation* becomes Equation 1. Although methods based upon the substitution of a *difference equation* for the differential equation usually necessitate considerable work to obtain the desired results, they have the advantage of being applicable to any shape of body, any assumption in regard to boundary conditions, or any variation in the coefficient of diffusivity.

Methods of procedure for solving the *difference equation*, usually for the analogous problem of heat-flow, may be found in the literature*.

After a solution for the distribution of shrinkage tendency at a given time has been obtained to the desired accuracy, there still remains the problem of solving for stresses. This may be done by graphical analysis, as illustrated by Buchanan and Schroeder[16] if the problem is one-dimensional or by more elaborate means if the problem is two- or three-dimensional.†

SUMMARY OF THE THEORETICAL DEVELOPMENT

The theoretical equations for the flow of heat are used for the unrestrained shrinkage of concrete. Unrestrained shrinkage is defined as the unit linear contraction that would occur in an element if it were unrestrained by neighboring elements. This is not the same as unit shortening (commonly called shrinkage) of a so-called unrestrained specimen. Having developed expressions for unrestrained shrinkage for each of three different conditions (Cases I, II and III), equations for shortening, warping, and stresses were derived.

The equations for two conditions—slab or beam drying from one face only, Case I, and slab or beam drying from two opposite faces, Case II—were found to be very much alike in form. However, the equation for shrinkage stress in the slab or beam drying from one surface contains an additional term, $\left(6 - 12\,\frac{g}{b}\right)\frac{2Eb\epsilon_{max}}{3b^2}$, that is not in the corresponding

*See, for example, References 14 and 15.
†See, for example, References 17, 18, and 19.

equation for a slab or beam drying from two opposite surfaces. Computations show that the equation with the added term gives much less stress for the same size of body and the same period of drying. Compare Tables 6 and 5.

Equations are given for all the stresses in a prism drying from all four surfaces, the third condition treated. These equations, though rather complicated in appearance, can be readily evaluated if the desired accuracy is such that only a few terms in each series need be considered. For a rather rough approximation of the stress that is usually the most important in this third condition, the comparatively simple equation $\sigma_z = E(S - S_{av})$ is recommended.

Tables and curves are given from which the theoretical shrinkages, stresses, etc., may be obtained, at any point in the specimen after any period of drying, for various values of the physical properties, diffusivity, surface factor, ultimate shrinkage, and dimensions of the specimen.

Examples are given showing how numerical values may be computed from the equations and how the tables and curves may be used.

REFERENCES

1. "Drying Shrinkage of Large Concrete Members," by R. W. Carlson, ACI JOURNAL, Jan.-Feb. 1937, *Proc.* V. 33, p. 327.

2. *Higher Mathematics for Engineers and Physicists*, by I. S. and E. S. Sokolnikoff, McGraw-Hill Book Co., New York, N. Y., 2d Ed., 1941, p. 368.

3. *Theory of Elasticity*, by S. Timoshenko, McGraw-Hill, New York, 1934, p. 196.

4. "Theorie der Setzung von Tonschichten," by K. v. Terzaghi and O. K. Fröhlich, Franz Deuticke, Leipzig und Wien, 1936.

5. "Calculation of Temperature Distribution in a Succession of Lifts Due to Release of Chemical Heat," by R. E. Glover, ACI JOURNAL, Nov.-Dec. 1937, *Proc.*. V. 34, p. 105.

6. "The Drying of Porous Solids," by A. B. Newman, Interim Publication, Am. Inst. of Chem. Eng., Aug. 1, 1931.

7. "Flow of Heat in Dams," by R. E. Glover, ACI JOURNAL, Nov.-Dec. 1934, *Proc.* V. 31, p. 113.

8. Reference (3), p. 31.

9. "Application of the Fourier Method to the Solution of Certain Boundary Problems in the Theory of Elasticity," by G. Pickett, *J. Applied Mechanics*, Sept. 1944, V. 11, No. 3, p. A-176.

10. "The Buckling Load for a Rectangular Plate with Four Clamped Edges," G. I. Taylor, *Zeitschrift fur Angewandte Mathematic und Mechanic*, V. 13, 1933, pp. 147-152.

11. *Theory of Plates and Shells*, by S. Timoshenko, McGraw-Hill, New York, 1940, pp. 222-232.

12. Ref. (3), pp. 21-23.

13. "The Effect of Biot's Modulus on Transient Thermal Stresses in Concrete Cylinders," by G. Pickett, *Proc.* Am. Soc. Testing Materials, V. 39, 1939, p. 913.

14. "A Simple Method for the Computation of Temperatures in Concrete Structures," by R. W. Carlson, ACI JOURNAL, Nov.-Dec. 1937, *Proc.* V. 34, p. 89.

15. "Resistance to Cracking of Surface Layer of Concrete Gravity Dams," by G. A. Nielaender, *Second Congress on Large Dams*, Washington, D. C., 1936, V. 3, p. 417.

16. "Crazing on Concrete Building Stone," by J. E. Buchanan and W. Schroeder. Bulletin No. 3. Engr. Exp. Station, Univ. of Idaho Bulletin, Vol. XXVII, No. 16, Aug. 1932.

17. *Relaxation Methods in Engineering Science*, by R. V. Southwell, Oxford Univ. Press, 1940.

18. "A Lattice Analogy for the Solution of Stress Problems," by Douglas McHenry, *J. Inst. of Civil Engrs.*, Dec. 1943, pp. 59-82.

19. "Numerical and Graphical Method of Solving Two-Dimensional Stress Problems," by H. Poritsky, H. D. Snively, and C. R. Wylie, Jr., *J. Applied Mechanics*, June 1939, V. 6, No. 2, p. A-63.

20. "The Effect of Change in Moisture-Content on the Creep of Concrete under a Sustained Load," by G. Pickett, ACI JOURNAL, Feb. 1942, *Proc.* V. 38, p. 333.

21. "Die Beeinflussung des Schwindens von Portlandzement durch Sulfate," by G. Haegermann, *Zement 28* (40) 599 (1939).

22. "A New Aspect of Creep in Concrete and Its Application to Design," by Douglas McHenry, Proc. Am. Soc. Testing Materials, V. 43, 1943, p. 1069.

23. "Attempts to Measure the Cracking Tendency of Concrete," by R. W. Carlson, ACI JOURNAL, June, 1940, *Proc.* V. 36, p. 533.

24. "The Influence of Gypsum on the Hydration and Properties of Portland Cement Pastes," by W. Lerch, unpublished.

25. "The Dependence of the Shrinkage of Portland Cement on Physical and Chemical Influences," by H. Kühl and D. H. Lu, *Tonind. Z. 59* (70) 843 (1935).

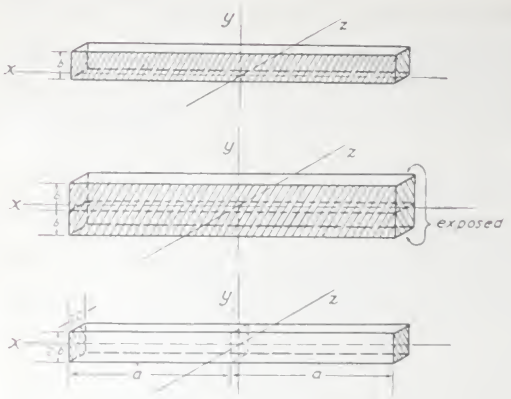

Fig. 1—Illustrations of the conditions treated. Shading indicates sealed surfaces. Case I—Beam (or slab) drying from one face only. Case II—Beam (or slab) drying from two opposite faces. Case III—Prism drying from four faces. The ends of the prism at $x = \pm a$ are sealed.

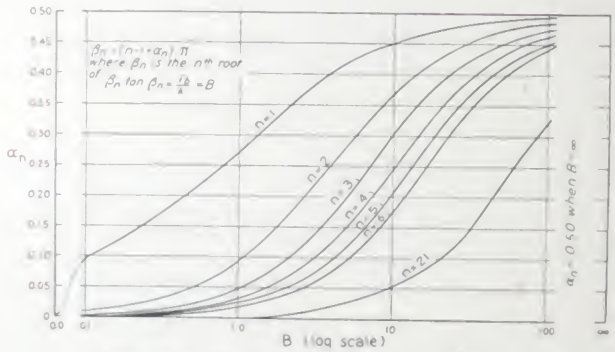

Fig. 2—Curves for the determination of β_n

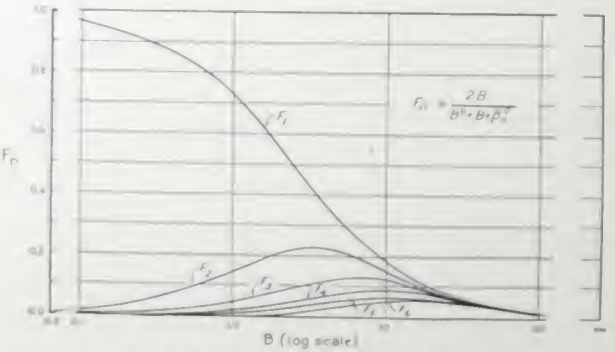

Fig. 3—Relationship between F_n and B

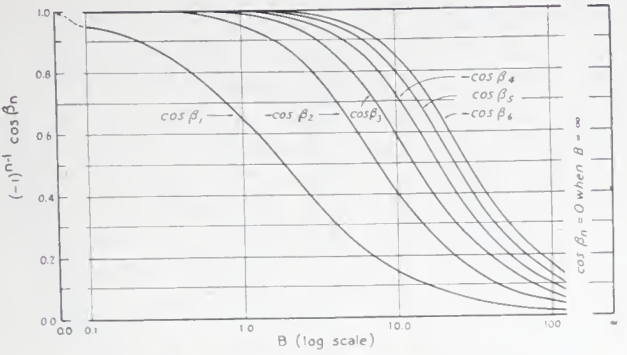

Fig. 4—Relationship between cos β_n and B

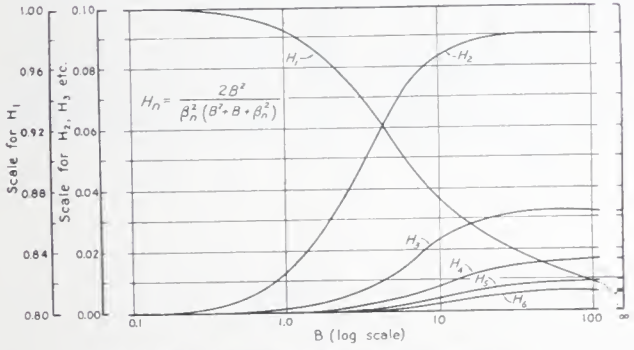

Fig. 5—Relationship between H_n and B

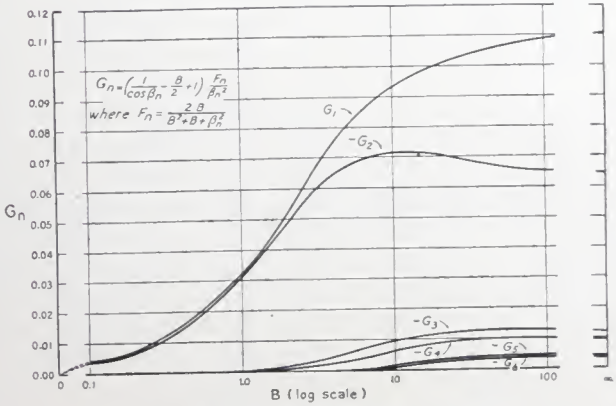

Fig. 6—Relationship between G_n and B

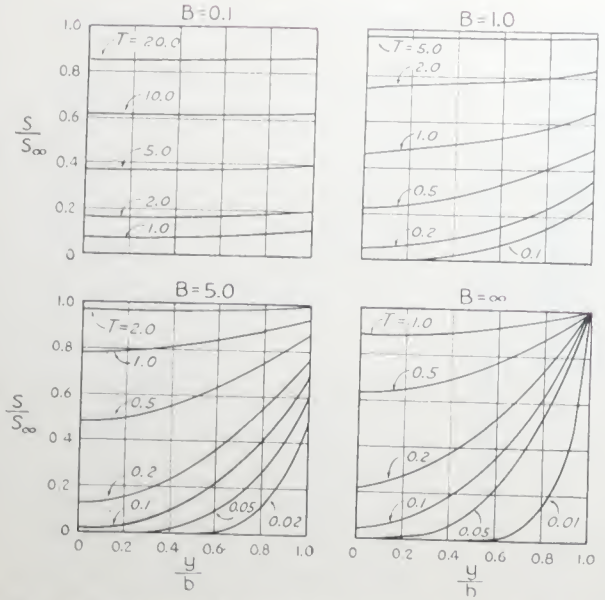

Fig. 7—Distribution of shrinkage for various values of B and T

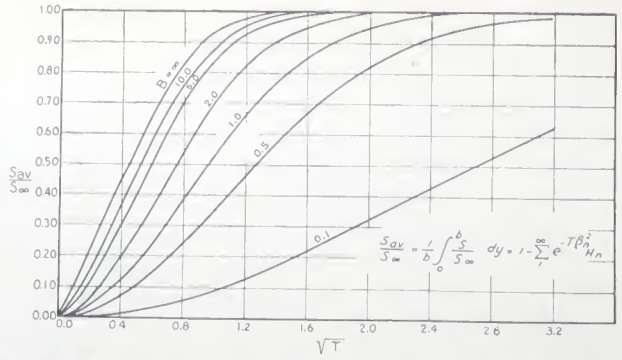

Fig. 8—Theoretical curves showing the ratio of unit shortening to final shortening vs. the square root of the time parameter

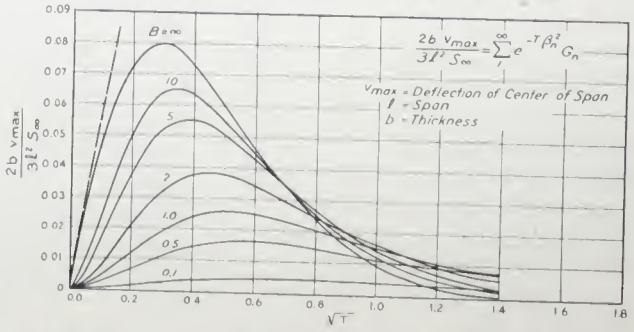

Fig. 9—Theoretical curves showing warping vs. square root of the time parameter for a prism drying from one side

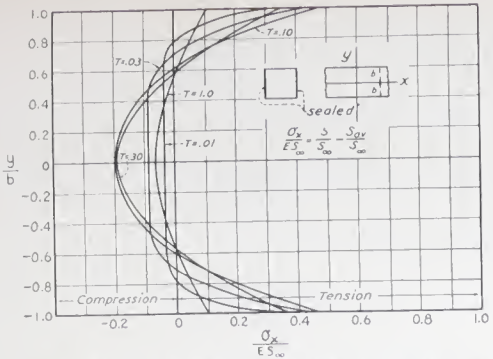

Fig. 10—Theoretical distribution of stresses at various values of T for Case II (or Case I where warping is prevented). $B = 5.0$

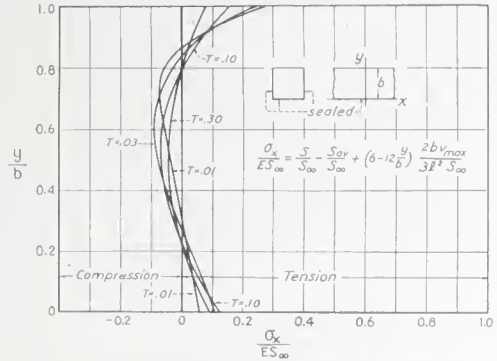

Fig. 11—Theoretical distribution of stress at various values of T for Case I. $B = 5.0$

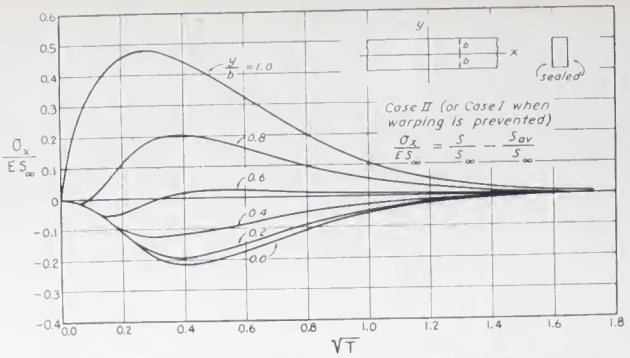

Fig. 12—Stress vs. square root of T at various distances from central plane of prisms drying from two opposite sides. $B = 5.0$

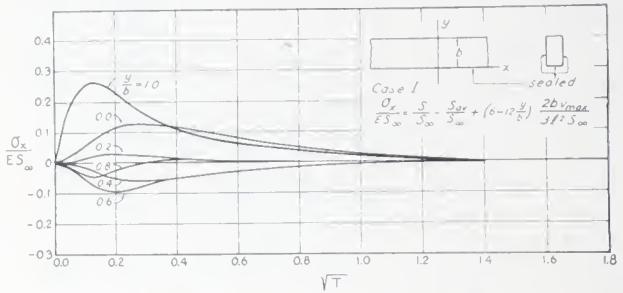

Fig. 13—Stress vs. square root of T at various values of y/b for an unrestrained prism drying from only one surface. $B = 5.0$

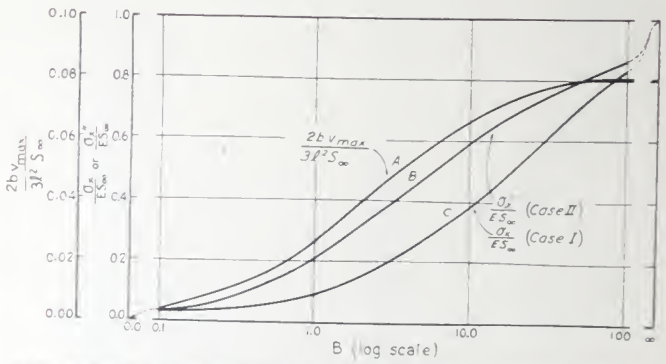

Fig. 14—Maximum stress (maximum value of stress at exposed surface) and maximum warping vs. the parameter B

TABLE 1—β_n

$\beta_n \tan \beta_n = B$

B	β_1	β_2	β_3	β_4	β_5	β_6
0.0	0	π	2π	3π	4π	5π
0.1	0.311053	3.1731	6.2991	9.4354	12.574	15.715
0.5	0.653271	3.2923	6.3615	9.4774	12.606	15.740
1.0	0.860334	3.4256	6.4372	9.5292	12.645	15.771
2.0	1.076874	3.6436	6.5783	9.6296	12.722	15.834
5.0	1.31384	4.0338	6.9097	9.8927	12.935	16.010
10.0	1.42886	4.3058	7.2281	10.200	13.213	16.260
100.0	1.55525	4.6656	7.7760	10.887	13.998	17.109
∞	$\pi/2$	$3\pi/2$	$5\pi/2$	$7\pi/2$	$9\pi/2$	$11\pi/2$

TABLE 2—RATIO OF SHRINKAGE (OR SWELLING) TO ULTIMATE SHRINKAGE (OR SWELLING)

$$\frac{S}{S_u} = 1 - \Sigma e^{-T\beta_n^2} F_n \frac{\cos \beta_n \frac{y}{h}}{\cos \beta_n}$$

T	$\frac{y}{h}=0$	$\frac{y}{h}=0.2$	$\frac{y}{h}=0.4$	$\frac{y}{h}=0.6$	$\frac{y}{h}=0.8$	$\frac{y}{h}=1.0$	$\frac{y}{h}=0$	$\frac{y}{h}=0.2$	$\frac{y}{h}=0.4$	$\frac{y}{h}=0.6$	$\frac{y}{h}=0.8$	$\frac{y}{h}=1.0$
	$\beta=0.1$						$\beta=1.0$					
0.0	0	0	0	0	0	0	0	0	0	0	0	0
0.005	.0001	.0000	.0000	.0000	.0002	.0000	.0001	.0000	.0000	.0000	.0002	.0000
0.010	.0003	.0001	.0001	.0001	.0003	.0001	.0002	.0000	.0000	.0000	.0003	.0000
0.015	.0005	.0001	.0001	.0001	.0004	.0001	.0003	.0000	.0000	.0000	.0004	.0000
0.020	.0006	.0001	.0001	.0001	.0005	.0001	.0004	.0000	.0000	.0000	.0005	.0000
0.030	.0009	.0001	.0001	.0001	.0007	.0001	.0006	.0000	.0000	.0000	.0007	.0000
0.040	.0011	.0001	.0001	.0001	.0008	.0001	.0008	.0000	.0000	.0000	.0008	.0000
0.050	.0013	.0001	.0001	.0001	.0009	.0001	.0010	.0000	.0000	.0000	.0009	.0000
0.060	.0015	.0001	.0001	.0001	.0010	.0001	.0012	.0000	.0000	.0000	.0010	.0000
0.070	.0017	.0001	.0001	.0001	.0011	.0001	.0014	.0000	.0000	.0000	.0011	.0000
0.10	.0023	.0001	.0001	.0001	.0013	.0001	.0019	.0000	.0000	.0000	.0013	.0000
0.15	.0033	.0001	.0001	.0001	.0015	.0001	.0028	.0000	.0000	.0000	.0015	.0000
0.20	.0043	.0001	.0001	.0001	.0016	.0001	.0037	.0000	.0000	.0000	.0016	.0000
0.30	.0060	.0001	.0001	.0001	.0017	.0001	.0052	.0000	.0000	.0000	.0017	.0000
0.40	.0075	.0001	.0001	.0001	.0017	.0001	.0065	.0000	.0000	.0000	.0017	.0000
0.50	.0088	.0001	.0001	.0001	.0017	.0001	.0077	.0000	.0000	.0000	.0017	.0000
0.60	.0100	.0001	.0001	.0001	.0017	.0001	.0088	.0000	.0000	.0000	.0017	.0000
0.70	.0111	.0001	.0001	.0001	.0017	.0001	.0098	.0000	.0000	.0000	.0017	.0000
1.0	.0144	.0001	.0001	.0001	.0017	.0001	.0127	.0000	.0000	.0000	.0017	.0000
1.5	.0198	.0001	.0001	.0001	.0017	.0001	.0175	.0000	.0000	.0000	.0017	.0000
2.0	.0245	.0001	.0001	.0001	.0017	.0001	.0217	.0000	.0000	.0000	.0017	.0000
3.0	.0324	.0001	.0001	.0001	.0017	.0001	.0287	.0000	.0000	.0000	.0017	.0000
4.0	.0388	.0001	.0001	.0001	.0017	.0001	.0344	.0000	.0000	.0000	.0017	.0000
5.0	.0441	.0001	.0001	.0001	.0017	.0001	.0391	.0000	.0000	.0000	.0017	.0000
7.0	.0522	.0001	.0001	.0001	.0017	.0001	.0463	.0000	.0000	.0000	.0017	.0000
10.0	.0601	.0001	.0001	.0001	.0017	.0001	.0533	.0000	.0000	.0000	.0017	.0000
13.0	.0659	.0001	.0001	.0001	.0017	.0001	.0584	.0000	.0000	.0000	.0017	.0000
20.0	.0753	.0001	.0001	.0001	.0017	.0001	.0667	.0000	.0000	.0000	.0017	.0000
	$\beta=3.0$						$\beta=\infty$					
0.0	0	0	0	0	0	0	0	0	0	0	0	0
0.001	.0000	.0000	.0000	.0000	.0000	.1330	.0000	.0000	.0000	.0000	.0000	.1600
0.002	.0000	.0000	.0000	.0000	.0001	.2060	.0000	.0000	.0000	.0000	.0000	.1600
0.005	.0000	.0000	.0000	.0000	.0002	.3210	.0000	.0000	.0000	.0000	.0000	.1600
0.010	.0000	.0000	.0000	.0000	.0005	.4564	.0000	.0000	.0000	.0000	.0000	.1600
0.015	.0000	.0000	.0000	.0000	.0007	.5579	.0000	.0000	.0000	.0000	.0000	.1600
0.020	.0000	.0000	.0000	.0000	.0010	.6379	.0000	.0000	.0000	.0000	.0000	.1600
0.030	.0000	.0000	.0000	.0000	.0014	.7592	.0000	.0000	.0000	.0000	.0000	.1600
0.040	.0000	.0000	.0000	.0000	.0018	.8454	.0000	.0000	.0000	.0000	.0000	.1600
0.050	.0000	.0000	.0000	.0000	.0021	.9098	.0000	.0000	.0000	.0000	.0000	.1600
0.070	.0000	.0000	.0000	.0000	.0027	.9997	.0000	.0000	.0000	.0000	.0000	.1600
0.10	.0000	.0000	.0000	.0000	.0034	1.0938	.0000	.0000	.0000	.0000	.0000	.1600
0.15	.0000	.0000	.0000	.0000	.0042	1.1938	.0000	.0000	.0000	.0000	.0000	.1600
0.20	.0000	.0000	.0000	.0000	.0047	1.2600	.0000	.0000	.0000	.0000	.0000	.1600
0.30	.0000	.0000	.0000	.0000	.0052	1.3338	.0000	.0000	.0000	.0000	.0000	.1600
0.40	.0000	.0000	.0000	.0000	.0054	1.3717	.0000	.0000	.0000	.0000	.0000	.1600
0.50	.0000	.0000	.0000	.0000	.0055	1.3938	.0000	.0000	.0000	.0000	.0000	.1600
0.70	.0000	.0000	.0000	.0000	.0056	1.4138	.0000	.0000	.0000	.0000	.0000	.1600
1.0	.0000	.0000	.0000	.0000	.0056	1.4238	.0000	.0000	.0000	.0000	.0000	.1600
1.5	.0000	.0000	.0000	.0000	.0056	1.4238	.0000	.0000	.0000	.0000	.0000	.1600
2.0	.0000	.0000	.0000	.0000	.0056	1.4238	.0000	.0000	.0000	.0000	.0000	.1600
3.0	.0000	.0000	.0000	.0000	.0056	1.4238	.0000	.0000	.0000	.0000	.0000	.1600
4.0	.0000	.0000	.0000	.0000	.0056	1.4238	.0000	.0000	.0000	.0000	.0000	.1600

TABLE 3—UNIT SHORTENING—AVERAGE UNIT SHRINKAGE $\left(\frac{S_{av}}{S_\infty}\right)$

$$\frac{S_{av}}{S_\infty} = 1 - \sum_{1}^{\infty} e^{-T\beta^2_n} H_n$$

T	$B = 0.1$	$B = 0.5$	$B = 1.0$	$B = 2.0$	$B = 5.0$	$B = 10.0$	$B = \infty$
0.001	0.0001	0.0005	0.0010	0.0019	0.0045	0.0080	0.0357
0.002	0.0002	0.0010	0.0019	0.0037	0.0085	0.0147	0.0506
0.003	0.0003	0.0015	0.0029	0.0055	0.0124	0.0206	0.0619
0.005	0.0005	0.0024	0.0047	0.0090	0.0196	0.0323	0.0800
0.010	0.0010	0.0048	0.0093	0.0173	0.0370	0.0556	0.1129
0.015	0.0015	0.0072	0.0137	0.0252	0.0515	0.0755	0.1383
0.02	0.0020	0.0095	0.0181	0.0317	0.0649	0.0932	0.1596
0.03	0.0030	0.0141	0.0265	0.0473	0.0891	0.1242	0.1954
0.04	0.0039	0.0185	0.0347	0.0611	0.1115	0.1512	0.2257
0.05	0.0049	0.0231	0.0426	0.0742	0.1319	0.1753	0.2523
0.075	0.0074	0.0340	0.0620	0.1050	0.1779	0.2282	0.3090
0.10	0.0098	0.0446	0.0803	0.1336	0.2186	0.2739	0.3506
0.15	0.0146	0.0653	0.1154	0.1860	0.2895	0.3510	0.4370
0.20	0.0193	0.0854	0.1489	0.2327	0.3510	0.4167	0.5041
0.30	0.0288	0.1239	0.2064	0.3190	0.4555	0.5258	0.6133
0.40	0.0382	0.1606	0.2666	0.3939	0.5422	0.6136	0.6979
0.50	0.0474	0.1957	0.3188	0.4604	0.6148	0.6849	0.7641
0.75	0.0702	0.2771	0.4339	0.5962	0.7498	0.8109	0.8726
1.0	0.0924	0.3502	0.5296	0.6979	0.8375	0.8865	0.9313
1.5	0.1353	0.4751	0.6751	0.8306	0.9315	0.9591	0.9800
2.0	0.1761	0.5767	0.7756	0.9052	0.9711	0.9857	0.9942
3.0	0.2521	0.7233	0.8930	0.9625	0.9949	0.9981	0.9995
4.0	0.3211	0.8182	0.9489	0.9907	0.9991	0.9998	1.0000
5.0	0.3837	0.8821	0.9756	0.9971	0.9998	1.0000	
7.5	0.5161	0.9594	0.9962	0.9998	1.0000		
10.0	0.6301	0.9860	0.9994	1.0000			
15.0	0.7658	0.9983	1.0000				
20.0	0.8556	0.9998					

TABLE 4—WARPING $\left(\frac{2b\,v_{max}}{3l^2 S_\infty} \text{ in thousandths}\right)$

$$\frac{2b\,v_{max}}{3l^2\,S_\infty} = \sum_{1}^{\infty} e^{-T\beta^2_n} G_n$$

T	$B = 0.1$	$B = 0.5$	$B = 1.0$	$B = 2.0$	$B = 5.0$	$B = 10.0$	$B = \infty$
0	0	0	0	0	0	0	0
0.0010	0.048	0.235	0.46	0.91	2.13	3.82	16.83
0.0015	0.071	0.348	0.68	1.33	3.08	5.43	19.79
0.0020	0.093	0.458	0.90	1.73	3.99	6.89	23.22
0.0030	0.137	0.674	1.32	2.54	5.73	9.61	27.90
0.0040	0.180	0.883	1.72	3.31	7.23	12.03	31.66
0.0050	0.222	1.008	2.12	4.03	8.69	14.27	34.89
0.0075	0.324	1.579	3.06	5.74	13.68	19.16	41.36
0.010	0.421	2.045	3.94	7.35	15.18	23.35	46.42
0.015	0.606	2.920	5.59	10.25	20.45	30.38	54.12
0.020	0.778	3.735	7.08	12.92	24.97	35.92	59.78
0.030	1.092	5.415	9.74	17.34	32.63	44.71	67.67
0.040	1.375	6.518	12.05	21.07	38.32	50.93	72.80
0.050	1.628	7.832	14.03	24.21	42.70	55.33	76.15
0.075	2.161	10.138	17.96	30.08	49.98	62.22	79.76
0.10	2.568	11.846	20.75	33.87	53.81	65.16	80.40
0.15	3.126	14.017	23.96	37.56	55.70	64.50	74.18
0.20	3.457	15.128	25.29	38.32	53.89	60.56	66.85
0.30	3.757	15.773	25.61	36.28	47.03	50.52	52.74
0.40	3.843	15.546	24.14	32.88	39.90	41.38	41.27
0.50	3.851	15.043	22.59	29.43	33.64	33.77	32.25
0.75	3.782	13.588	18.85	22.07	21.86	20.27	17.40
1.0	3.694	12.217	15.67	16.52	14.20	12.17	9.39
1.5	3.519	9.869	10.82	9.25	5.99	4.38	2.74
2.0	3.353	7.959	7.47	5.18	2.53	1.58	0.80
3.0	3.044	5.203	3.57	2.05	0.45	0.20	0.07
4.0	2.763	3.417	1.70	0.51	0.08	0.03	0.01
5.0	2.508	2.216	0.81	0.16	0.01	0.00	0.00
7.5	1.969	0.763	0.13	0.01	0.00		
10.0	1.506	0.262	0.02	0.00			
15.0	0.953	0.031	0.00				
20.0	0.587	0.004					

TABLE 5—RATIO OF STRESS σ''_x IN AN UNRESTRAINED BEAM DRYING FROM TWO OPPOSITE SIDES (OR IN A BEAM DRYING FROM ONLY ONE SIDE AND RESTRAINED AGAINST WARPING) TO THE ULTIMATE STRESS FOR COMPLETE RESTRAINT ES_∞

$$\frac{\sigma''_x}{ES_\infty} = \frac{S}{S_\infty} - \frac{S_{av}}{S_\infty}$$

T	$\frac{y}{b}=0$	$\frac{y}{b}=0.2$	$\frac{y}{b}=0.4$	$\frac{y}{b}=0.6$	$\frac{y}{b}=0.8$	$\frac{y}{b}=1.0$	$\frac{y}{b}=0$	$\frac{y}{b}=0.2$	$\frac{y}{b}=0.4$	$\frac{y}{b}=0.6$	$\frac{y}{b}=0.8$	$\frac{y}{b}=1.0$
	$B=0.1$						$B=1.0$					
0.0	0	0	0	0	0	0	0	0	0	0	0	0
0.005	-.0005	-.0005	-.0005	-.0005	-.0003	.0075	-.0047	-.0047	-.0047	-.0047	-.0040	.0703
0.010	-.0010	-.0010	-.0010	-.0010	-.0001	.0102	-.0093	-.0093	-.0093	-.0091	.0000	.0942
0.015	-.0015	-.0015	-.0015	-.0014	.0006	.0120	-.0137	-.0137	-.0137	-.0125	.0059	.1101
0.020	-.0020	-.0020	-.0020	-.0017	.0013	.0138	-.0181	-.0181	-.0176	-.0148	.0124	.1235
0.030	-.0030	-.0030	-.0029	-.0019	.0027	.0162	-.0265	-.0264	-.0252	-.0170	.0246	.1425
0.040	-.0039	-.0039	-.0036	-.0019	.0041	.0183	-.0346	-.0344	-.0314	-.0165	.0353	.1563
0.050	-.0049	-.0048	-.0042	-.0019	.0051	.0198	-.0423	-.0416	-.0361	-.0152	.0444	.1670
0.075	-.0072	-.0069	-.0054	-.0014	.0072	.0228	-.0599	-.0570	-.0442	-.0104	.0616	.1851
0.10	-.0090	-.0084	-.0061	-.0009	.0090	.0249	-.0735	-.0682	-.0486	-.0054	.0735	.1961
0.15	-.0117	-.0106	-.0069	.0000	.0114	.0277	-.0910	-.0821	-.0531	.0014	.0871	.2064
0.20	-.0133	-.0119	-.0074	.0005	.0126	.0293	-.0990	-.0880	-.0539	.0056	.0929	.2081
0.30	-.0149	-.0132	-.0079	.0010	.0138	.0306	-.1028	-.0900	-.0530	.0089	.0948	.2027
0.40	-.0154	-.0136	-.0081	.0011	.0141	.0308	-.0975	-.0855	-.0497	.0091	.0894	.1893
0.50	-.0154	-.0135	-.0080	.0013	.0142	.0311	-.0914	-.0801	-.0463	.0088	.0838	.1766
0.75	-.0152	-.0133	-.0079	.0013	.0139	.0302	-.0764	-.0669	-.0386	.0074	.0699	.1471
1.0	-.0148	-.0130	-.0077	.0012	.0136	.0295	-.0634	-.0555	-.0321	.0062	.0582	.1222
1.5	-.0140	-.0123	-.0072	.0011	.0131	.0281	-.0439	-.0384	-.0223	.0042	.0401	.0844
2.0	-.0134	-.0118	-.0070	.0011	.0124	.0267	-.0303	-.0266	-.0153	.0029	.0277	.0583
3.0	-.0122	-.0107	-.0063	.0010	.0113	.0243	-.0145	-.0127	-.0074	.0013	.0131	.0277
4.0	-.0111	-.0097	-.0057	.0009	.0102	.0221	-.0069	-.0060	-.0035	.0007	.0063	.0133
5.0	-.0101	-.0089	-.0052	.0008	.0092	.0200	-.0032	-.0028	-.0016	.0004	.0030	.0064
7.5	-.0079	-.0069	-.0041	.0006	.0073	.0157						
10.0	-.0061	-.0055	-.0033	.0005	.0055	.0120						
15.0	-.0038	-.0033	-.0020	.0003	.0035	.0076						
20.0	-.0023	-.0021	-.0012	.0002	.0022	.0047						
	$B=5.0$						$B=\infty$					
0.0	0	0	0	0	0	0	0	0	0	0	0	0
0.001	-.0045	-.0045	-.0045	-.0045	-.0045	.1514	-.0357	-.0357	-.0357	-.0357	-.0357	.9743
0.002	-.0085	-.0085	-.0085	-.0085	-.0084	.2010	-.0506	-.0506	-.0506	-.0506	-.0490	.9494
0.005	-.0196	-.0196	-.0196	-.0196	-.0124	.2823	-.0800	-.0800	-.0800	-.0799	-.0345	.9200
0.010	-.0370	-.0370	-.0370	-.0362	.0020	.3473	-.1129	-.1129	-.1127	-.1069	.0412	.8871
0.015	-.0515	-.0515	-.0515	-.0467	.0255	.3863	-.1383	-.1383	-.1378	-.1174	.1100	.8617
0.020	-.0649	-.0646	-.0645	-.0523	.0483	.4120	-.1596	-.1595	-.1569	-.1141	.1577	.8404
0.030	-.0890	-.0881	-.0848	-.0538	.0871	.4441	-.1953	-.1944	-.1810	-.0929	.2188	.8046
0.040	-.1109	-.1098	-.0998	-.0481	.1176	.4609	-.2249	-.2210	-.1918	-.0684	.2538	.7743
0.050	-.1299	-.1277	-.1094	-.0401	.1404	.4707	-.2492	-.2408	-.1945	-.0464	.2748	.7477
0.075	-.1709	-.1604	-.1207	-.0200	.1765	.4778	-.2892	-.2683	-.1874	-.0073	.2966	.6910
0.10	-.1965	-.1796	-.1230	-.0044	.1948	.4727	-.3096	-.2789	-.1771	.0151	.3011	.6494
0.15	-.2169	-.1969	-.1189	-.0130	.2052	.4484	-.3012	-.2644	-.1531	.0317	.2790	.5630
0.20	-.2164	-.1897	-.1112	-.0199	.1996	.4175	-.2765	-.2404	-.1331	.0343	.2517	.4959
0.30	-.1918	-.1671	-.0948	.0216	.1749	.3551	-.2200	-.1906	-.1048	.0292	.1986	.3867
0.40	-.1634	-.1422	-.0801	.0191	.1485	.2995	-.1723	-.1492	-.0818	.0231	.1554	.3021
0.50	-.1379	-.1193	-.0674	.0163	.1253	.2522	-.1347	-.1166	-.0640	.0180	.1214	.2359
0.75	-.0896	-.0779	-.0437	.0106	.0814	.1638	-.0727	-.0629	-.0345	.0097	.0655	.1273
1.0	-.0582	-.0506	-.0284	.0069	.0529	.1064	-.0393	-.0341	-.0187	.0052	.0353	.0687
1.5	-.0246	-.0214	-.0170	.0029	.0223	.0448	-.0114	-.0100	-.0054	.0015	.0103	.0200
2.0	-.0104	-.0090	-.0051	.0012	.0094	.0189	-.0034	-.0029	-.0016	.0004	.0030	.0058
3.0	-.0019	-.0016	-.0009	.0002	.0016	.0033						

TABLE 6—RATIO OF STRESS σ_x IN AN UNRESTRAINED BEAM DRYING FROM ONLY ONE SIDE TO ULTIMATE STRESS FOR COMPLETE RESTRAINT ES_∞

$$\frac{\sigma_x}{ES_\infty} = \frac{S}{S_\infty} - \frac{S_{av}}{S_\infty} + (6 - 12\,\frac{y}{b})\,\frac{2bv_{max}}{3l^2S_\infty}$$

T	$\frac{y}{b}=0$	$\frac{y}{b}=0.2$	$\frac{y}{b}=0.4$	$\frac{y}{b}=0.6$	$\frac{y}{b}=0.8$	$\frac{y}{b}=1.0$	$\frac{y}{b}=0$	$\frac{y}{b}=0.2$	$\frac{y}{b}=0.4$	$\frac{y}{b}=0.6$	$\frac{y}{b}=0.8$	$\frac{y}{b}=1.0$
	$B = 0.1$						$B = 1.0$					
0.0	0	0	0	0	0	0	0	0	0	0	0	0
0.005	.0008	.0003	-.0002	-.0008	-.0011	.0062	.0080	.0029	-.0022	-.0072	-.0116	.0576
0.010	.0015	.0005	-.0005	-.0015	-.0016	.0078	.0143	.0049	-.0046	-.0138	-.0142	.0706
0.015	.0021	.0007	-.0008	-.0021	-.0016	.0084	.0198	.0064	-.0070	-.0192	-.0142	.0766
0.020	.0027	.0008	-.0011	-.0026	-.0015	.0091	.0243	.0074	-.0091	-.0233	-.0131	.0811
0.030	.0036	.0009	-.0016	-.0032	-.0012	.0096	.0319	.0087	-.0135	-.0287	-.0105	.0841
0.040	.0044	.0011	-.0019	-.0036	-.0009	.0100	.0377	.0090	-.0169	-.0310	-.0081	.0840
0.050	.0048	.0011	-.0022	-.0039	-.0008	.0100	.0419	.0089	-.0193	-.0320	-.0061	.0828
0.075	.0058	.0009	-.0028	-.0040	-.0006	.0098	.0479	.0077	-.0226	-.0320	-.0031	.0773
0.10	.0064	.0008	-.0031	-.0040	-.0002	.0095	.0510	.0065	-.0237	-.0303	-.0012	.0716
0.15	.0071	.0007	-.0031	-.0038	.0001	.0089	.0528	.0042	-.0243	-.0274	.0008	.0626
0.20	.0074	.0005	-.0033	-.0036	.0002	.0085	.0527	.0030	-.0236	-.0247	.0019	.0564
0.30	.0076	.0003	-.0034	-.0035	.0003	.0080	.0509	.0022	-.0223	-.0218	.0026	.0490
0.40	.0077	.0002	-.0035	-.0035	.0003	.0077	.0473	.0014	-.0207	-.0199	.0025	.0445
0.50	.0077	.0004	-.0034	-.0033	.0002	.0077	.0441	.0012	-.0192	-.0183	.0025	.0318
0.75	.0075	.0003	-.0034	-.0032	.0003	.0075	.0367	.0010	-.0160	-.0152	.0020	.0340
1.0	.0074	.0003	-.0033	-.0032	.0003	.0073	.0306	.0009	-.0133	-.0126	.0018	.0282
1.5	.0071	.0004	-.0030	-.0031	.0004	.0070	.0210	.0006	-.0093	-.0088	.0011	.0195
2.0	.0067	.0003	-.0030	-.0029	.0003	.0066	.0145	.0003	-.0063	-.0061	.0008	.0135
3.0	.0061	.0003	-.0026	-.0027	.0003	.0060	.0069	.0002	-.0031	-.0030	.0002	.0063
4.0	.0055	.0002	-.0025	-.0024	.0003	.0055	.0033	.0001	-.0015	-.0013	.0002	.0031
5.0	.0049	.0001	-.0022	-.0022	.0002	.0050	.0017	.0001	-.0006	-.0006	.0001	.0015
7.5	.0039	.0001	-.0017	-.0020	.0002	.0039						
10.0	.0030	.0001	-.0014	-.0014	.0001	.0030						
15.0	.0019	.0001	-.0009	-.0008	.0001	.0019						
20.0	.0012	.0000	-.0005	-.0005	.0001	.0012						
	$B = 5.0$						$B = \infty$					
0.0	0	0	0	0	0	0	0	0	0	0	0	0
0.001	.0083	.0032	-.0019	-.0071	-.0122	.1386	.0653	.0249	-.0155	-.0559	-.0963	.8733
0.002	.0154	.0059	-.0037	-.0133	-.0288	.1771	.0887	.0330	-.0227	-.0785	-.1326	.8101
0.005	.0325	.0117	-.0092	-.0300	-.0437	.2302	.1293	.0456	-.0381	-.1218	-.1601	.7107
0.010	.0541	.0176	-.0188	-.0544	-.0526	.2562	.1656	.0542	-.0570	-.1626	-.1259	.6086
0.015	.0712	.0221	-.0270	-.0712	-.0481	.2636	.1864	.0565	-.0729	-.1823	-.0848	.5370
0.020	.0849	.0250	-.0345	-.0822	-.0413	.2622	.1991	.0557	-.0852	-.1858	-.0575	.4817
0.030	.1068	.0294	-.0456	-.0930	-.0304	.2483	.2109	.0493	-.0998	-.1741	-.0249	.3984
0.040	.1190	.0282	-.0538	-.0941	-.0204	.2310	.2119	.0411	-.1044	-.1558	-.0083	.3375
0.050	.1263	.0260	-.0582	-.0913	-.0133	.2145	.2080	.0335	-.1031	-.1378	.0005	.2905
0.075	.1290	.0195	-.0607	-.0800	-.0034	.1779	.1896	.0190	-.0916	-.1031	.0093	.2122
0.10	.1264	.0141	-.0584	-.0690	.0011	.1498	.1728	.0105	-.0806	-.0814	.0117	.1670
0.15	.1173	.0072	-.0521	-.0538	.0047	.1142	.1439	.0027	-.0641	-.0573	.0119	.1179
0.20	.1069	.0043	-.0465	-.0448	.0056	.0942	.1233	.0001	-.0529	-.0459	.0112	.0951
0.30	.0904	.0022	-.0384	-.0348	.0056	.0729	.0962	-.0009	-.0416	-.0340	.0089	.0705
0.40	.0760	.0014	-.0322	-.0288	.0049	.0601	.0753	-.0006	-.0323	-.0264	.0068	.0545
0.50	.0639	.0011	-.0270	-.0241	.0042	.0534	.0588	-.0006	-.0253	-.0207	.0053	.0424
0.75	.0416	.0008	-.0175	-.0156	.0027	.0326	.0318	-.0002	-.0135	-.0111	.0029	.0230
1.0	.0270	.0005	-.0114	-.0101	.0018	.0212	.0170	-.0002	-.0074	-.0061	.0015	.0124
1.5	.0113	.0002	-.0098	-.0043	.0007	.0089	.0050	.0000	-.0021	-.0018	.0004	.0036
2.0	.0048	.0001	-.0021	-.0018	.0003	.0037	.0014	.0000	-.0006	-.0006	.0001	.0010
3.0	.0008	.0000	-.0004	-.0003	.0000	.0006						

Title 42-8 —a part of PROCEEDINGS, AMERICAN CONCRETE INSTITUTE Vol. 42

JOURNAL
of the
AMERICAN CONCRETE INSTITUTE
(copyrighted)

Vol. 17 No. 4 7400 SECOND BOULEVARD, DETROIT 2, MICHIGAN February 1946

Shrinkage Stresses in Concrete*

By GERALD PICKETT†
Member American Concrete Institute

PART 2—APPLICATION OF THE THEORY PRESENTED IN PART 1 TO EXPERIMENTAL RESULTS

Carlson's results on prisms drying from one end

As mentioned in Part 1, Carlson[1] applied diffusion principles to the problem of computing both loss of moisture and distribution of shrinkage. The fundamental equations on which his computations were based are the equations to which Equations 5 and 22 of Part 1 reduce when the parameter B is set equal to infinity. In his experimental work the prisms were allowed to dry through one end only, the rest of the surface being sealed. Measurements were made over gage lines that were parallel to the direction of flow of moisture. These conditions appear to be most favorable for the direct measurement of the distribution of shrinkage tendency since in an unrestrained specimen shrinkage stresses should not have any appreciable effect on the unit shortening in the direction of moisture flow.

In Fig. 3 of his paper Carlson showed two diagrams. One diagram gave the distribution of shrinkage as measured after a definite period of drying and the other gave the computed "distribution of drying" (loss of moisture) for different assumed coefficients of diffusion for the same period of drying. The observed distribution of shrinkage and the computed "distribution of drying" are in good agreement when the proper coefficient is selected. However, as shown by Fig. 1 of his paper, the measured loss in weight was not in very good agreement with the theory. Carlson could have obtained slightly better agreement between theory and measured shrinkage if he had taken surface conditions into account,

*Part 1 of this paper was published in the ACI Journal, January, 1946, and includes (p. 194) the complete list of references.

†Professor of Applied Mechanics, Kansas State College, Manhattan, Kan., formerly Portland Cement Association Research Laboratory, Chicago.

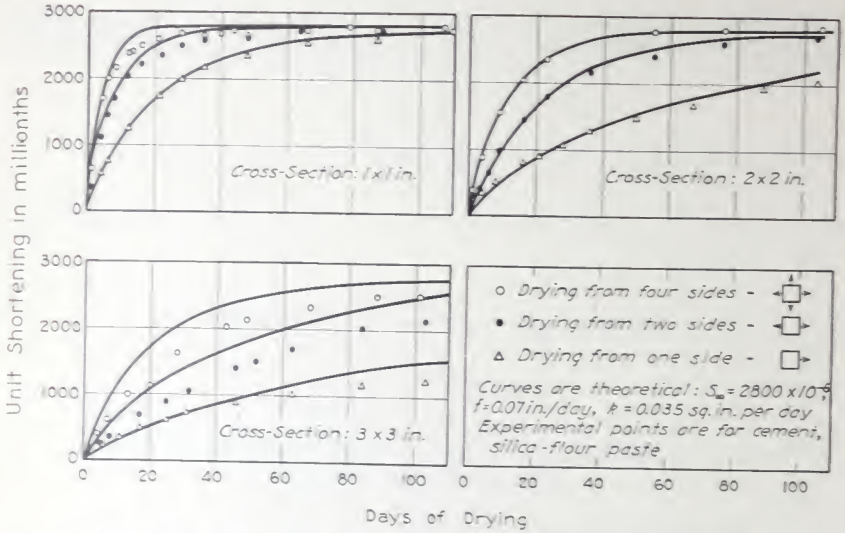

Fig. 15—Comparison of observed and calculated course of shrinkage

i.e., used a finite value for the parameter B. However, had he done so, the discrepancy between theory and measured loss in weight would have been greater than that shown.

Carlson's work is important evidence in support of the hypothesis that shrinkage of concrete approximately follows the laws of diffusion.

Shrinkage of prisms of various sizes drying from one or more sides

In the work done in this laboratory measurements were made on gage lengths transverse to the direction of moisture flow. Since variations in shrinkage along the path of moisture flow result in stresses transverse to the direction of flow, the measurements include the strains produced by these stresses. If, however, the specimens are long compared to their dimension in the direction of moisture flow and the stress-strain relation is linear, then as shown in Part I the shortening of the central axis will be equal to the average shrinkage. The results to be discussed provide a test of the theory for conditions in which both size of specimen and number of exposed sides are variable.

Fig. 15 shows the unit shortening versus days of drying for three different sizes of prisms made of the same mix and for the three different drying conditions discussed in Part 1. Mix A and cement M, described in the Appendix, were used. The specimens were cured seven days under water. Each point is the average of the results from two prisms. The curves were constructed from computations based on the theoretical equations developed in Part 1. These equations, which give the theoreti-

cal relationship between unit shortening, the constants of the material, and dimensions of the specimen have the form

$$\text{unit shortening} = S_{av} = F\left(S_\infty, \frac{fb}{k}, \frac{kt}{b^2}, \frac{c}{b}\right)$$

where S_∞ is ultimate shrinkage for the assumed final drying, f is the surface factor, k is the diffusivity factor, and b and c are dimensions of the specimen. The exact form of the function, especially the way in which c/b enters into it, differs with the drying condition.

The three constants S_∞, f, and k were evaluated from average experimental values for the pair of prisms of 2-in. square cross-section, drying from four exposed sides. From these same constants the curves were constructed, as shown in Fig. 15, not only for this pair but also for the theoretical unit shortening of the other eight pairs of prisms. The agreement between the experimental values and the calculated curves is fairly satisfactory except for two pairs of 3x3-in. specimens, which were observed to have cracked during drying and therefore could not be expected to shorten in accordance with the theory.

Discussion of the validity of the theory on the basis of the foregoing data

The data from those specimens that did not crack, together with the data given by Carlson, might seem to indicate rather conclusively that shrinkage does take place in accordance with the theory developed in Part 1. However, such a conclusion would not be justified. A good fit between an equation and experimental data is necessary but it is not sufficient proof of a theory. Although constants in the equations of Part 1 may be chosen so that the theory given there will be in good agreement with experiment for certain measurements on specimens under a few different conditions, the theory should be expected to fail under some other conditions since it rests on some assumptions that are not wholly correct. Shrinkage is not linearly related to change in moisture content; the flow of moisture in concrete does not follow the law of diffusion; and the stress-strain relation is not linear. Since the assumptions are not wholly correct, the factors S_∞, f, k, and E that are supposed to characterize the material must be empirical, and experimentally determined numerical values of these factors will be different for different tests on the same material. The good agreement between theory and the experimentally determined contraction of the specimens discussed above must be the result of the balancing of opposing effects. They will not necessarily balance the same way in another test.

The foregoing criticism means that however promising the theory may appear from the results of a few experiments, the application of the theory must be limited and extrapolation of the results to sizes of specimens or conditions of drying other than those for which the constants

were determined cannot be made with confidence. The selection of these constants for given conditions constitutes the chief difficulty for the practical use of the equations. This does not mean that the theory is of little value; we believe it to be of considerable value.

True, the theoretical equations are not rigorously correct and the constants cannot have exactly the meaning attached to them. But the evidence is that shrinkage does follow the diffusion equation approximately and that the deformations and stresses are approximately those given by the theoretical equations if the empirical constants selected are such as to give fair agreement with experimental results.

Although the experimental results shown in Fig. 15 appear to be in good agreement with the theory, a close study shows the following in regard to those prisms drying from only one side: (1) After one or two months of drying the shortening of the prisms drying from one side becomes progressively less than that indicated by the theoretical curves. (2) The experimental results from the 2x2-in. prisms deviate more from the computed values than do those of 1x1-in. cross-section. (The 1x1-in. specimens drying from one side have the same b-values as the 2x2-in. specimens from which the constants S_∞, f, and k were determined.) (3) The 3x3-in. prisms drying from one side deviate still more from the computed values than do those of 2x2-in. cross-section. It is expected that extrapolation to still larger sizes would result in still greater discrepancies between experimental and computed values unless allowance is made for change in the constants with change in b-value.

Comparison of data on warping with data on shortening

A more critical test of the theory is provided by the results shown in Fig. 16. The abscissa for these diagrams is the square root of the period of drying divided by the thickness of the prism.* As mentioned in Part 1, using square-root-of-time as the abscissa gives a nearly straight line for an appreciable portion of plots of both shortening and warping. Dividing the square root of time by the thickness of the specimen puts all specimens on a more nearly comparable basis. Multiplying the warping (deflection of center of a 32-in. span) by the thickness puts the "free warping" specimens on the same basis in regard to unit deformation.

The plotted points in the upper diagram of Fig. 16 represent the shortening of those prisms of Fig. 15 that were drying from only one side. The points in the lower diagram represent the warping of the specimens made of the same kind of concrete, also drying from only one side. Although these two sets of data were not obtained on the same specimens at the same time, they are representative of what is obtained when both sets of measurements are made simultaneously on the same specimens.

*The dimension in the direction of drying is taken as the thickness.

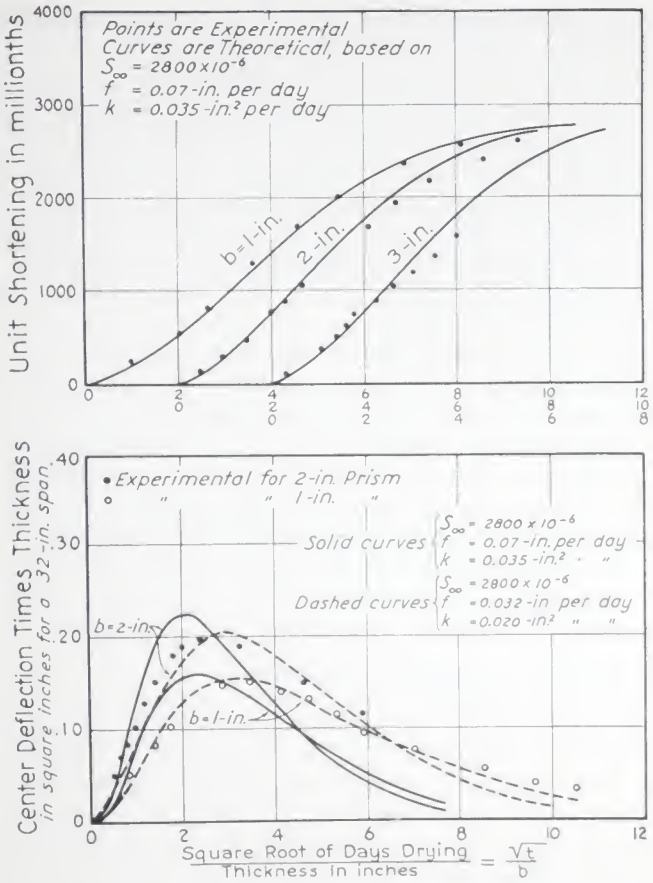

Fig. 16—Comparison of observed and calculated course in shortening and warping of prisms of mix A and cement M

The curves in the upper diagram and the solid curves in the lower diagram were constructed from the theoretical equations using the same values of the constants S_∞, f, and k as were used in constructing the curves of Fig. 15. Therefore, the three curves in the upper diagram of Fig. 16 represent the same equations as three of the curves in Fig. 15; they differ only in the abscissas. The solid curves in the lower diagram deviate considerably from the plotted points. This indicates even greater disagreement with theory than is shown in Fig. 15. However, the dashed curves obtained from the theoretical equation by using the same value of S_∞ but with f reduced by 54 per cent and k reduced by 43 per cent are in very good agreement with the experimental values.

The computed shrinkage stresses will be about the same whether the first or the reduced values of f and k are used.

The values of the constants S_∞, f, and k, used in constructing the dashed curves, were obtained from three measurements as follows: (1) maximum warping of the 1-in. specimen, (2) time at which this maximum warping occurred, and (3) final shortening of a companion specimen. The agreement throughout the course of drying between the experimental values for warping and those given by the theoretical equations when these constants are used is excellent for the 1-in. specimen and very good for the 2-in. specimen.

The above shows that if data on warping and data on shortening are analyzed separately, either group of data will appear to be in accord with the theory if the thicknesses of the specimens do not differ too much, but the values of f and k obtained from the two groups of data will be different. The fact that the factor k is an empirical rather than a fundamental property of the material is believed to be the chief reason why both groups of data cannot be represented satisfactorily by one set of constants. The empirical nature of f is considered to be of only secondary importance in this study because it has much less effect than k on the shortening-vs.-time and warping-vs.-time relations.

Effect of differences in k on warping and shortening

The effects of differences in diffusivity on the theoretical values of warping (Equation 23)* and shortening (Equation 22)* are shown in Fig. 17 where these quantities are plotted against the parameter $\sqrt{ft/b}$ for three different relative values of k. As shown, differences in k have practically no effect on the early warping; each curve follows the same course until it approaches its maximum point. The lower k, the greater the maximum warping. This effect on maximum value of warping, of course, would be anticipated because of the effect of k through the parameter fb/k $(= B)$ as shown in Fig. 9.* As shown by the curves for shortening in Fig. 17, the effect of k upon shortening is entirely different from its effect on warping. The rate of shortening is materially reduced by a reduction in k, but the maximum shortening is unaffected.

This theoretical analysis of the different effects of changes in k on shortening and on warping has been useful in explaining differences in performances of concretes made with cements of different composition. For example, experimental results from concretes made with two different cements are shown in Fig. 18. Mix C was used. A comparison of Fig. 17 and 18 leads to the conclusion that the coefficient of diffusivity for concretes made with cement No. 5-1500-1.9 is lower than for con-

*See Part 1.

cretes made with cement No. 1-1500-1.9*. Concretes made with cement from clinker No. 5 shortened at a lower rate but according to data not plotted eventually shortened more than concretes from clinker No. 1.

Before this explanation was found, it seemed surprising that of two groups of specimens drying from one side only, subjected to the same exposure, one group would warp more and shorten less than the other group. In order that one specimen warp less than a second when the two specimens have the same average shrinkage, the distribution of shrinkage in the first specimen would have to be more nearly uniform. For the same surface conditions, a large value of k through the parameter fb/k, tends to make shrinkage more nearly uniform and therefore is accompanied by less warping. An increase in uniformity of shrinkage also reduces the shrinkage stresses in an unrestrained specimen and therefore reduces the tendency for spontaneous cracking. (Fig. 14 Part 1—shows how the theoretical maximum stresses depend on the parameter fb/k $(= B)$.)

Effect of alkali content on k and its possible effects on cracking

It had been observed from various laboratory tests designed to measure cracking tendencies that concretes made with cements from clinker No. 5 tended to crack more than those made with cement from clinker No. 1, even though measurements often showed less volume change at the end of a given period of drying for the concretes of clinker No. 5. This greater cracking tendency of cement from clinker No. 5 was attributed to its higher alkali content, since this appeared to be the only important difference in their chemical compositions. Attempts to evaluate k for concretes made with cements from these two clinkers showed that for the same mix proportions the value of k for concrete made with the cement of higher-alkali content was only one-half that made with the cement of lower-alkali content. These observations suggested the possibility that: alkali reduced k, a reduced k resulted in higher shrinkage stresses, and higher stresses resulted in more cracking.

To investigate this effect of differences in alkali content more fully, several tests were made using cement No. 1-1665-2.48. The procedure was to add 0.91 per cent Na_2O by weight of cement in the form of $NaOH$ to the mixing water of one of two companion mixes. The results of one test using mix B are shown in Fig. 19 where shortening and weight losses of prisms are plotted against period of drying.

The dimensions of the prisms were $2\frac{1}{2}$x$2\frac{1}{2}$x$11\frac{1}{4}$ in. They dried from all surfaces except the ends. By using for the specimens containing added alkali a time-scale equal to one-third the scale used for the regular specimens the corresponding curves for both sets of specimens approxi-

*As explained in the Appendix, the first number is the clinker number, the second is the specific surface (Wagner method), and the third is the percentage of SO_3.

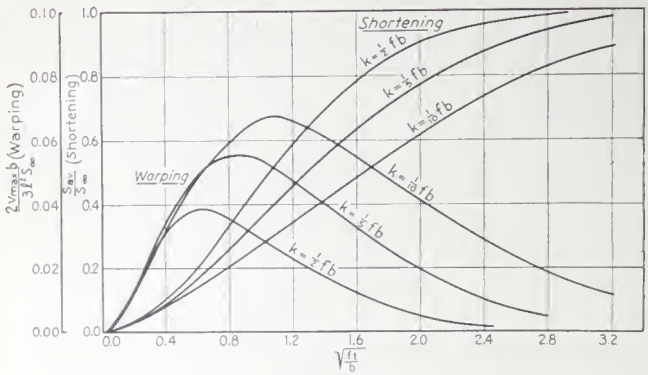

Fig. 17—Theoretical effect of k on the course of contraction and warping of prisms drying from one side only

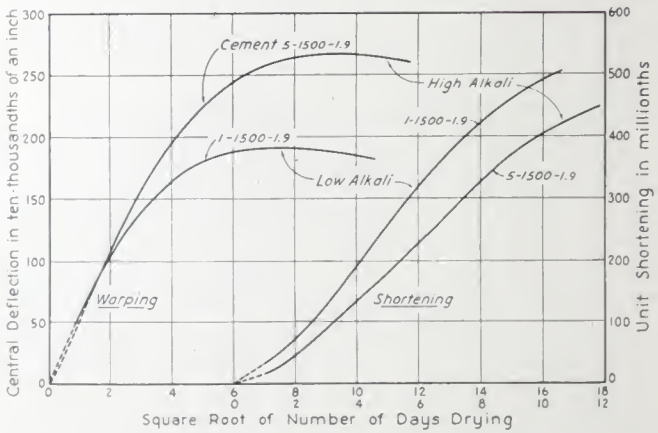

Fig. 18—Warping and shortening of prisms that differ primarily in the alkali content of the cement used

Prisms 3-in. thick in the direction of moisture travel. Deflection measured over a 32-in. span. Mix C. Cured 7 days.

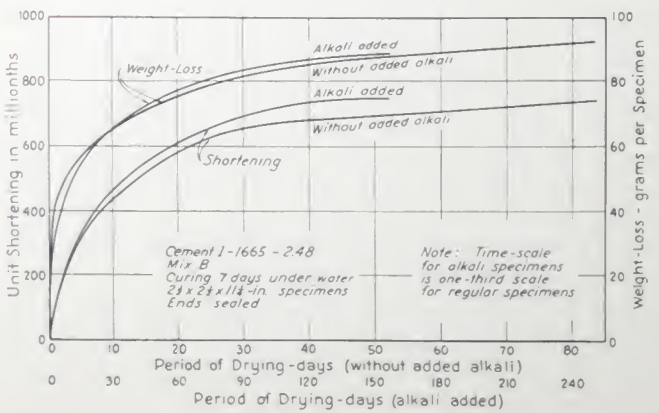

Fig. 19—Shrinkage and weight-loss for specimens with and without added alkali

mately coincided, indicating that the main effect of the added alkali was to reduce the diffusivities for both shrinkage and moisture flow to one-third the value without added alkali.

The effect of added alkali in reducing the diffusivity of shrinkage for cement of clinker No. 1 is in accord with data reported by Haegermann.[21] Haegermann was primarily interested in the effects on shrinkage of additions of various sulfates to cements of different C_3A contents. The sulfates tried were ferrous, calcium, magnesium, sodium, and potassium. The amounts added were such as to increase the SO_3, content 1 per cent, based on the cement. Five cements ranging from 15 per cent computed C_3A content to zero per cent C_3A were investigated.

The data were presented by Haegermann in the form of curves. For each cement, the curves representing the sodium and potassium sulfate additions are of noticeably different shape from the other curves for the same cement, the difference in shape being such as would result from a lower diffusivity. Since Haegermann did not give data on loss in weight during drying, it can only be inferred from the data on shrinkage that the sodium and potassium sulfates also reduced the diffusivity of moisture flow.

From theoretical consideration, it appears that any highly soluble material should reduce the relative rate of drying; i.e., should increase the time required to lose a given percentage of the total amount of moisture to be lost.* However, since many other factors affect the rate of shrinkage, and alkalies have many other effects which may indirectly affect shrinkage, one should expect many real and apparent contradictions to the above indication that an increase in alkali content will retard shrinkage.

The effect of the added alkali on cracking was investigated by means of the "wedge test"† and by the "restrained-shrinkage test" (subsequently described). The result was that specimens of higher alkali content showed a much greater tendency to crack, as measured by these tests.

Other tests made in this laboratory show that for cements containing an appreciable percentage of tricalcium aluminate, an increase in alkali content will increase final shrinkage of laboratory specimens unless the increase in alkali is accompanied by an increase in gypsum. The greater

*This reasoning is based on the supposition that at least part of the flow of water in concrete is by means of the following cycle: evaporation at an air-water interface, vapor diffusion across air space, capillary flow in liquid filled space, and again evaporation at air-water interface. Since the diffusivity of the soluble material within the liquid is finite rather than infinite, at any air-water interface at which water is evaporating, the concentration of soluble material will be higher than that for equilibrium with the adjacent liquid and thereby tend to restrict evaporation at this interface, and at any air-water interface at which water is condensing the concentration of soluble material will be lower than that for equilibrium with the adjacent liquid and thereby tend to restrict condensation at this interface. Therefore any highly soluble material should retard the drying by reducing the diffusivity of moisture flow.

†A specimen is cast in the form of a wedge and, after curing, is permitted to dry from the two non-parallel surfaces.

tendency to crack of the specimens with higher alkali content might have been due, at least in part, to a decrease in diffusivity and an increase in final shrinkage.

On the other hand, the possible benefits from alkali should not be overlooked. The lowered rate of moisture loss will permit the interior of concrete to retain sufficient moisture for additional hydration for a longer time after drying of the surface begins. Prevention of complete drying of the interior during the usual drying season should be especially advantageous in preventing cracking when restraints against shortening are present. Tests in this laboratory have also shown that concretes of higher alkali content have greater capacity for plastic flow, which is a favorable property.

Decrease in k as drying proceeds

As drying proceeds, the value of the coefficient of shrinkage diffusivity k apparently decreases. This decrease no doubt results from a progressive decrease in the apparent diffusivity of moisture, diffusivity of moisture probably being a function of the moisture content. If diffusivity of moisture is a function of moisture content, then the shrinkage diffusivity can be considered to be a function of the shrinkage S and the differential equation becomes non-linear. Adding particular solutions, as was done in Part 1, is then not permissible.

However, if in place of considering k to be a function of the dependent variable S it is considered to be a function of the independent variable t and of the dimensions of the body, then the differential equation remains linear. Furthermore, if the factor f is considered to vary with time in a like manner so that the ratio f/k remains constant (see, for example, Equation 2a), then all of the equations for displacements, stresses and strains developed in Part 1 still apply if the symbol t appearing in them is replaced by a function of t and the dimensions. The changes suggested above amount to a continual change in the time-scale so that the time required for given conditions to develop becomes progressively longer. By modifying the theory in this way better agreement with experimental results can be obtained.

Fig. 20 is an example of applying the foregoing analysis. The plotted points are from experimental data on the average warping of four 3-in. specimens of concrete of mix B with cement 1-2280-1.94. When an attempt was made to select constant values of f, k, and S_∞ to be used in the theoretical equation that would give curves in agreement with all of the experimental values, not all the data could be brought into agreement with the theoretical equation. But by taking the following values for the factors, a better fit was obtained.

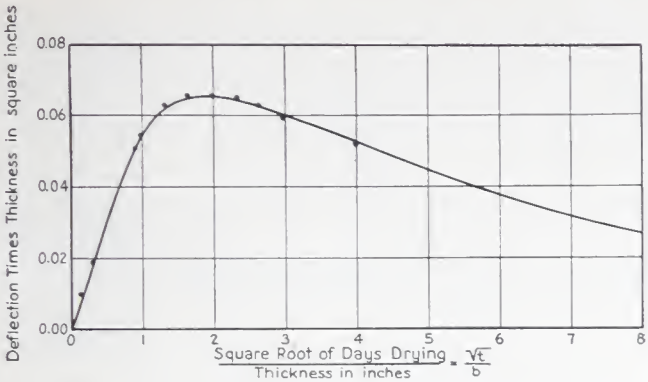

Fig. 20—Comparison of theoretical and experimental warping

Points are from the average warping of four 3-in beams. Span 32-inches. Mix B. Cement 1-2280 – 1.94. Cured 7 days.

$$k = 0.10 \sqrt{\frac{2}{2+t}} \text{ in}^2/\text{day}$$

$$f = 1.67\ k \text{ in/day, i.e., } \frac{fb}{k} = 5$$

$$S_\infty = 765 \times 10^{-6}$$

When these values are introduced into the differential equations and a solution made, the symbol T in the final equations for warping, etc., is replaced by

$$\frac{4k_o}{b^2}\left[\sqrt{\frac{2+t}{2}} - 1\right]$$

where k_o is the initial value of k or 0.10 sq. in. per day. For convenience in making computations preliminary to plotting of the theoretical curve, t was expressed in terms of T, or $t = \frac{b^2T}{k_o} + \frac{b^4T^2}{8k_o^2}$. The tabular values used for constructing the curve are given below:

From Table 4		Computed Values		
T	$\frac{2bv_{max}}{3l^2S_\infty}$	t	$\frac{\sqrt{t}}{b}$	$v_{max}b$
0.01	0.0152	1.00	0.333	0.0178
0.03	0.0326	3.61	0.635	0.0384
0.10	0.0538	19.1	1.46	0.0634
0.15	0.0557	36.4	2.01	0.0655
0.20	0.0539	58.5	2.55	0.0635
0.30	0.0470	118	3.62	0.0553
0.50	0.0336	298	5.75	0.0395
0.75	0.0219	639	8.41	0.0258

The better agreement that can be obtained by the modified theory probably would not compensate for the extra work in all cases. Since the

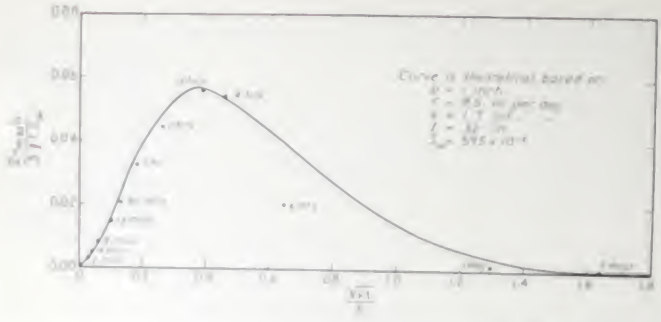

Fig. 21—Comparison of theoretical and experimental warping of beam absorbing moisture from one side

Points represent the warping of a 1-in. beam, having all but one of its surfaces sealed, during submersion in water. Cured 7 days and then dried at 50% R.H. for 10 months before testing. Mix B. Cement 1-2280-1.94. Span 32 inches.

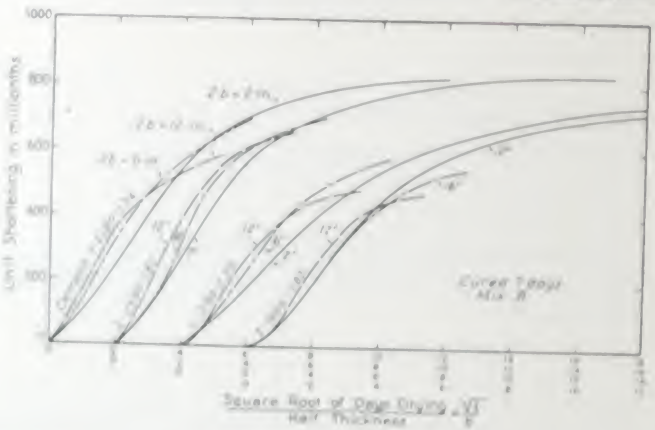

Fig. 22—Shrinkage of slabs of different thicknesses drying from two opposite sides

forms of the resulting differential equations, rather than the reasonableness of the assumption used, were given first consideration, the value of such modification is greatly reduced.

Warping of prisms during absorption of moisture from one side

Experimental results indicate that the theoretical equations are as applicable to the swelling of concrete as they are to the shrinking. However, the factors f and k are different; they are much larger than for shrinking if the exposed surface is submerged in water. Agreement between theory and experiment that is somewhat better in most respects than that usually found in absorption tests in this investigation is shown in Fig. 21. The plotted points give experimental values and the curve gives theoretical values for a 1-in. prism of concrete, mix B with cement 1-2280-1.94. The specimen, which had all surfaces sealed except one, had previously been dried at 50 per cent relative humidity for ten months. This specimen reached a maximum warp after about three hours' absorption of water and at the end of 24 hours had returned to approximately

zero warp where it remained for the rest of the test, a period of one month. The experimental value for the warp after 6 hours' exposure is considered to be in error. Other tests on 1-in. prisms did not show the indicated large decrease in warp between the fourth and sixth hours of exposure.

Although the amount of experimental data on swelling is yet small, the indications are that the application of the theory as developed in Part 1 is limited, first, because at the beginning of wetting the moisture already present will ordinarily not be uniformly distributed; second, because of having remained wet longer, the cement in the interior regions will have hydrated more than that closer to the drying surface; and third, as the concrete becomes wet again, hydration again starts. Agreement with diffusion theory is not expected while hydration is occurring at an appreciable rate, especially if the formation of hydration products causes expansion.

Effect of thickness on rate and amount of shrinkage of walls or slabs

In an investigation of the effect of wall or slab thickness on the rate and amount of shrinkage the results shown in Fig. 22 were obtained. The specimens from which the data were taken were made of mix B. Cements of two different compositions and a fine and a coarse grind of each are represented. The specimens were cured seven days under water. The specimens were 34 inches long and of either 2x6- or 2x12-in. cross section. By sealing all but two surfaces the prisms were made to represent slabs or walls of 2-, 6-, and 12-in. thicknesses drying from two opposite sides. For example, the specimens that represented a wall 12 in. thick were 2x12x34-in. and dried from only the 2x34-in. surfaces, there being 12 inches between these surfaces.

Sets of gage-points were cast in these pseudo slabs so that the shortening over three or four 30-in. parallel gage lines could be measured on each specimen. Details are shown in the Appendix. Each curve was obtained by averaging the results from four specimens of a kind.

As shown in Fig. 22, the results from these concrete specimens are in general similar to those obtained on the cement-silica mix discussed previously (see upper diagram, Fig. 16.). The curves have the characteristic S-shape found for similar plotting of data from smaller specimens. The thicker the slab the greater its fb/k $(=B)$ and, according to theory as shown by Fig. 8 (of Part I), the greater the shortening should be for a given value of the abscissa, $\sqrt{t/b}$. The experimental data are partly in agreement and partly in disagreement with the theory in this regard. In the middle, straight-line portions of the curves, the curves are in the correct positions relative to each other, but in every case the relative positions become reversed at larger values of $\sqrt{t/b}$. Also, the relative

positions of the curves representing the two coarser grinds are reversed at the very beginning portion of the curves. This latter deviation from theory can be explained on the basis of a non-linear stress-flow relationship.

If the positive plastic flow* exceeds the negative, the specimen will not shorten as much as it would if plastic flow did not take place. Of course, if the total positive and negative flows are equal (algebraic average = zero), the length of the specimen is not changed by plastic flow and the algebraic average must be zero in an unrestrained specimen if the stress-flow relationship is linear. However, if the stress-flow relationship of the concrete is non-linear over the range of stresses developed, the flow increasing more rapidly than the first power of the stress, then, as explained in Ref. 20, shortening of the specimen is reduced by plastic flow. The reduction would be more pronounced for the thicker specimens (those of greater b) because, as shown by Curve B of Fig. 14 (Part I), an increase in the parameter fb/k ($=B$) results in an increase in the maximum stresses. The above explanation (on the basis of a non-linear stress-flow relationship) as to why the relative positions of the first parts of the curves representing the two coarser grinds were reversed from what they should be according to theory is not entirely satisfactory because the question arises as to why the curves representing the finer grinds were not reversed also. This point will be mentioned again and an additional explanation given in a later section after other tests with these concretes are reported.

The reversal in relative position of the curves beyond the straight-line portion is attributed to the lesser final shortening of thicker specimens and to the reduction in diffusivity as drying proceeds. The thicker the specimen the less the final shortening because:

(1) The very low rate of drying from the interior of thick specimens is favorable for continued hydration and additional hydration reduces shrinkage tendency.

(2) In a thicker specimen the region losing moisture at an appreciable rate is under greater restraint and for a longer time than in a thinner specimen; consequently, more inelastic elongation is developed.

Plastic flow

Before discussing further the results of measurements of plastic flow, certain common usages of the term will be explained. The term usually calls to mind permanent deformations of the infinitesimal elements of a body as a result of stresses. In many cases, especially if shrinkage-stresses or thermal stresses are present, neither the actual stresses nor the deformations produced by them are known.

*The term "plastic flow" is synonymous with the term "creep" as used by many writers. It is used for either tensile (positive) or compressive (negative) inelastic deformation. See the section on "Plastic Flow" for further explanation of the term.

In the usual measurements of plastic flow the quantity measured is the inelastic deformation of a body that results from applied loads. From these measurements computations are made of the inelastic deformations of the individual elements, i.e., average unit deformation if the load is axial or unit deformation of the outer fiber if the load produces flexure. If stresses from other sources are not present, the computed values may be representative of the actual plastic flow. But if stresses from other sources are present, the computed and actual values may differ appreciably. Therefore, if in addition to load stresses a specimen is under stress as a result of non-uniform temperature or non-uniform shrinkage, it should be made clear whether the term plastic flow refers to the resultant plastic flows of elements or to only computed plastic flows produced by loads. Since the effects of load and the effects of drying are not simply additive, there is no clear basis for deciding how much of the total deformation is due to the stresses arising directly from the load. In agreement with previous writers, the deformations produced by loads will be taken as the difference between the deformations of loaded specimens and the deformations of identical specimens under the same drying conditions but not under load. Only the deformations produced by loads will be computed and represented by curves, but in the *interpretation* of results consideration will be given to what the *actual* inelastic deformations are believed to be.

As shown by the formulas for plastic flow used in this paper, the total deformation produced by load is divided into two parts, elastic and inelastic. The elastic part is considered to be that which would be recovered immediately if the load were removed; it is determined from the computed load-stresses and the "dynamic" modulus of elasticity. The remaining part is considered to be the plastic flow produced by the load.

Some investigators make a slightly different division in that the elastic deformation is considered to be that which was produced immediately upon application of the load rather than that which would be recovered immediately upon removal of the load. The two values are equal if the modulus of elasticity does not change during the test. Some writers prefer to divide the total deformation produced by load into three parts: (1) that recovered immediately upon removal of load, (2) that not immediately but eventually recovered, (3) the permanent deformation. McHenry[22] restricts the use of the term plastic flow to the third part. This division into three parts has merit, especially for those cases in which the second part is an appreciable percentage of the total. For the data given in this paper no separation of the second and third parts could be made, but the permanent deformation (3) is believed to be much greater than the temporary (2).

If the specimen is not shrinking while it is under load, then a considerable part of the inelastic deformation is probably only temporary and apparently the result of viscous flow in the adsorbed water films. After removal of the load, the elastic constituents of the gel-structure tend to restore the original shape but are retarded by the viscosity of the adsorbed water films. However, if an elemental volume* of cement paste is shrinking while under stress, the conditions are different. The loss of moisture introduces relatively large interparticle forces which tend to change the relative positions of the colloidal particles within an element. Some adjacent particles are pulled closer together but others are moved further apart. During this time of movement the directions of relative motion of the particles may be appreciably affected by stresses on the element. In this way stresses on an element during the time it is shrinking may produce comparatively large permanent deformations.

The foregoing is one explanation for the much larger amount of plastic flow that a load will produce on a drying specimen compared to what it would produce if either the specimen were prevented from drying or had previously been dried. It is also an explanation of the relatively great capacity for the concrete near the drying surface to deform plastically without cracking. If the analysis is correct, then a definite stress-flow relationship cannot be ascribed to a given element of concrete since the amount of plastic flow would depend not only upon the magnitude and duration of stress on an element but also upon the changes in moisture content that occurred while the element was under stress.

Because most of the inelastic deformation was considered to be permanent and because the increase in deformation with time was considered to be controlled chiefly by changes in distribution of shrinkage and shrinkage-stresses with relatively small lag in time after the development of shrinkage-stress, the term "plastic flow" rather than "creep" was selected for the inelastic part of the deformation.

It is important to know in what way the pastic flows of the individual elements contribute to the inelastic deformations of the body as a whole. For example, if a body is under axial load the plastic flow in tension or compression caused by the load is the difference in the *algebraic sum* of the inelastic deformation of each element and what the algebraic sum would have been if the body had not been under load. But the plastic flow of a body under flexural load depends on the *moment* of the inelastic deformation of each element with respect to the "neutral axis." Both plastic elongation on the tension side and plastic compression on the compression side of a beam under flexural load contribute to the measured plastic flow of the beam as a whole.

*In this discussion non-homogeneity of the cement paste is recognized and an element of paste is not infinitesimal but large enough to be essentially like adjacent elements.

Summary of remarks on plastic flow. The actual plastic deformation of elemental volumes of a specimen may be much different from that computed on the basis of laboratory experiments if shrinkage-stresses are present, but in this paper the plotted curves represent such computed values. Computed values are based upon the difference in the deformations of loaded and not loaded specimens. The term "plastic flow" is used in this paper to refer to either actual or computed plastic deformation. Plastic deformation is arbitrarily defined as that part of the total deformation produced by stress (either by actual stress or by load-stress as indicated by the text) that would not be immediately recovered upon removal of the stress.

Effect of thickness on stresses and plastic flow when the slab is partially restrained against shortening

Companion specimens of the same size and sealed in the same manner as those represented in Fig. 22 were partially restrained against shrinkage by specially designed steel bars, somewhat as were those described by Carlson.[23] The main features of the steel bars are shown in Fig. 23. (The concrete specimen illustrated in Fig. 23, however, is from another test in which the concrete was allowed to dry from all sides and only one bar was used per specimen). Each specimen of 2x6-in. cross section contained two $\frac{5}{8}$-in. diameter bars, and each specimen of 2x12-in. cross section contained four $\frac{5}{8}$-in. diameter bars. The arrangement of bars is shown in the Appendix, and in Fig. 24.

A rubber tube covered the central 20 inches of each bar so as to prevent bond over a 20-in. gage length, thereby insuring the same axial force in the bar over all sections of the gage length. That part of each steel bar not covered with rubber was threaded and thus the bars were anchored to the concrete for a distance of 7 in. on each side of the gage length. Because of this anchorage the shortening of the steel bar over the gage length is equal to the shortening of the concrete over the same gage length. Moreover, as is obvious from considerations of equilibrium, the force in the concrete in this gage length is equal and opposite to the force in the steel in the same gage length. Therefore, the average unit stress in the concrete can be computed from the change in length, modulus of elasticity, and percentage of steel. The formula is

$$\sigma_c = \frac{A_s E_s}{A_c} \frac{\Delta l}{l}$$

where σ_c is average stress in the concrete
A_s is cross-sectional area of the steel
A_c is cross-sectional area of the concrete
E_s is Young's modulus for the steel

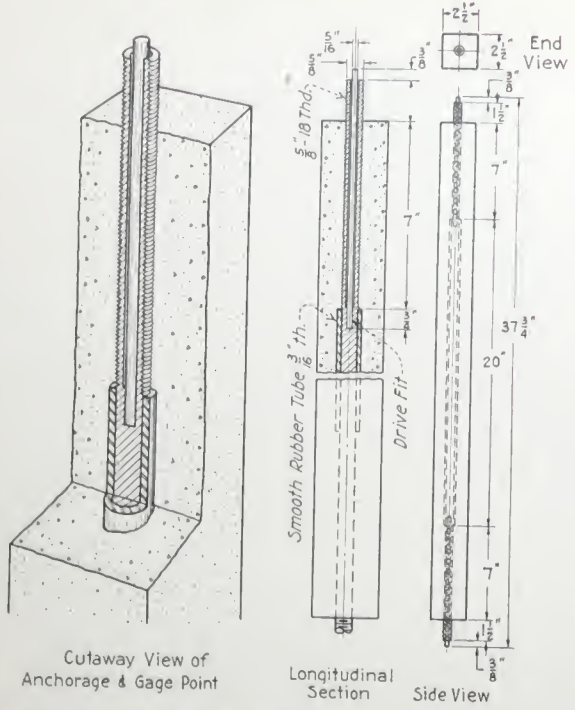

Fig. 23 (above)—Details of cracking—test specimen

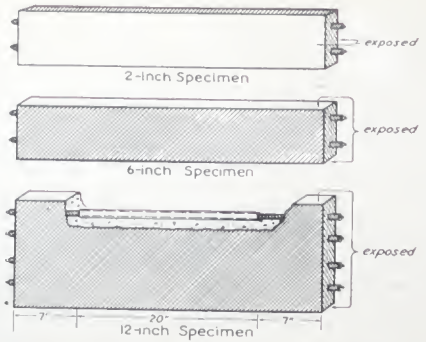

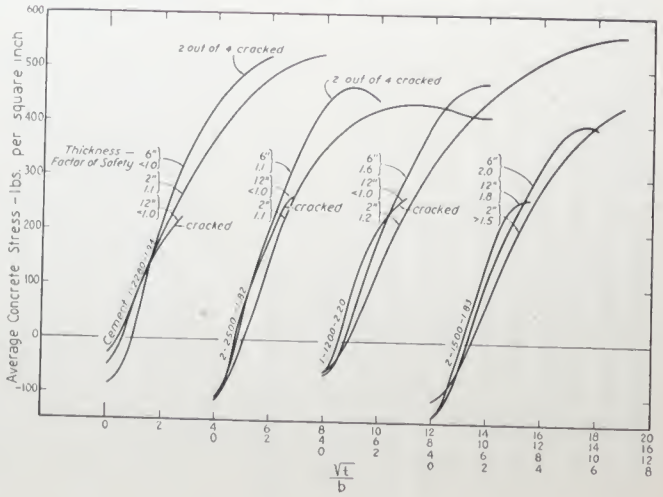

Fig. 24 (right)—Average stress in partially restrained specimens (each curve the average of four)

Δl is net change in length over gage length after corrections have been made for any change in temperature.* Δl is negative if the specimen has shortened.

l is gage length.

Not only the average stress caused by the restraint but also plastic flow caused by this stress can be computed if the modulus of elasticity of the concrete is known and the assumption is made that the shrinkage tendencies of the restrained specimens are the same as those for companion unrestrained specimens of the same size. The formula is

$$c = S_{av} - \frac{\sigma_c}{E_c} + \frac{\Delta l}{l}$$

where c is unit plastic flow caused by restraint,

S_{av} is the unit shortening of the free-shrinkage specimens, and

E_c is Young's modulus for the concrete.

Performance of partially restrained specimens. As explained in the Appendix all specimens were cured under water. The specimens tended to expand during this storage and consequently the concrete in those partially restrained with restraining bars was compressed. Therefore, for a short time after drying began, the direction of the plastic flow produced by the restraining bars was in a negative direction. Shortly after drying began, the stresses in the restraining bars changed from tensile to compressive, and the average stress in the concrete changed from compressive to tensile.

Under the conditions of this test the average stress reaches a maximum and then slowly decreases if failure by spontaneous cracking does not occur. A specimen's average stress and its shortening necessarily reach their maximums simultaneously if the temperature remains constant. Therefore, the time of maximum average stress is the time when the rate of average shrinkage equals the rate of plastic deformation. During the decrease of average stress, the rate of plastic deformation exceeds the rate of shrinking.

Ordinarily in this test the specimens are not permitted to reach a final equilibrium state in regard to shrinkage, shrinkage-stress, and plastic flow. But just after the maximum restraining force has been developed additional tensile load sufficient to cause failure of the specimen is applied. This load is applied to the protruding threaded ends of the restraining bars by a machine designed for the purpose. While the load is being applied, measurements are taken so that the added stress in the concrete can be determined. Further details are given in Fig. 33 of the Appendix.

*All tests were conducted in a room maintained at 76 ± 1°F and a relative humidity of 50 ± 2%, except for occasional deviations from these limits.

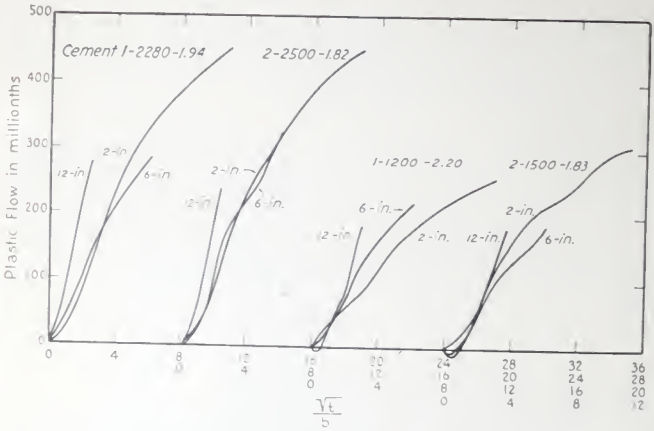

Fig. 25—Plastic flow in the partially restrained specimens of Fig. 24

Factor of safety. The purpose of the testing just described is to learn how close the specimen comes to cracking spontaneously. The ratio of the computed stress at failure to the maximum average shrinkage-stress is called a factor of safety. Specimens that crack spontaneously are reported as having a factor of safety less than unity. Results showing computed average shrinkage-stresses and plastic deformation are shown in Fig. 24 and 25, respectively. The record of the number of specimens of each cement that cracked spontaneously and of the average factors of safety (f.s.) of those that did not crack is also shown in Fig. 24.

Effect of thickness on plastic flow. Attention is called to the similarity of the three sets of curves in Fig. 22, 24, and 25. The similarity is not to be interpreted as necessarily indicating that the plastic deformation of an element is proportional to its stress. One is tempted to make this interpretation because, if it were true, then the plastic flow of a specimen would depend only on average stress and not on the distribution of stress. In general, the diagrams show that the 12-in. specimens developed considerably more plastic flow for the same amount of average stress than either the 2- or the 6-in. specimens.

There are several possible reasons for this: first, because of the lower rate of shortening, the larger specimens will have been under a given range of stress longer than the smaller specimens and therefore would be expected to have more plastic flow for the same stress. Since the time required for the same amount of shortening is approximately proportional to the square of the thickness, the 12-in. specimens will in general have been under a given range of stress about four times as long as the 6-in. specimens. Second, since the thicker specimens will have higher maximum stresses, the additional plastic flow could be accounted for by a non-linear stress-flow relationship whether or not this relationship

for each element was modified while the element was losing moisture rapidly. Third, the assumption that shrinkage tendencies of the restrained-shrinkage and free-shrinkage specimens are equal is not entirely correct and consequently their computed plastic flow are in error. A difference in the shrinkage tendencies of the 12-in. free and restrained specimens might result since the arrangement of the four bars was such as partially to obstruct the flow of moisture.

Probably all factors listed above contributed to the results. Of the factors causing the computed plastic flow to be greater in the 12-in. specimens, the author is of the opinion that the non-linear stress-flow relation contributed much more than the difference in duration of given stresses.* That the maximum stresses in the larger specimens are higher is shown by the fact that all the 12-in. restrained specimens of three of the four cements cracked (see Fig. 24) whereas only a few of the 6-in. specimens and none of the 2-in. specimens cracked.

According to most of these arguments the 2-in. specimens should have less plastic flow than the 6-in. specimens, whereas in general they have slightly more for the same shortening and for the same average stress. A complete explanation for this is not at hand, but the lesser extent of hydration of the cement in the 2-in. specimens because of their more rapid drying may be a factor. Also, the exposed surfaces of the 2-in. specimens were the top and bottom surfaces as cast, whereas the drying surfaces for all the other specimens were the sides as cast. Bleeding and settlement of the plastic mix before initial hardening is complete always makes the concrete near the top and that near the bottom as cast different from that at the sides. It must also be remembered that the computed plastic deformation may be more or less than the real plastic deformation of the material.

Use of beams drying from only one side for determining probable stresses in slabs or walls drying from two opposite sides

To obtain information on plastic flow and on the magnitude and distribution of stresses in unrestrained walls or slabs drying from two opposite sides another set of specimens, also companion to those represented in Fig. 22, were made. These specimens differed from those of Fig. 22 in that they were permitted to dry from only one side instead of two opposite sides and in that the thicknesses of corresponding specimens were just half those of Fig. 22. Since they were half as thick and dried from only one side instead of two sides (see Appendix), any one of these specimens was considered to have the same conditions of drying and consequently the same distribution of shrinkage tendency as either half of a corresponding specimen represented in Fig. 22.

*Most contemporary writers on the inelastic properties of concrete apparently would take the opposite view. This difference in viewpoint is explained and an argument for the author's view is given in Ref. 20.

If the distribution of shrinkage tendency is the same and if the correct external forces are applied so as to make all the deformations the same as those of either half of the corresponding specimen, then the distribution of stresses will also be the same.

Eight specimens of a kind were made, four of which were allowed to warp freely and four were restrained against warping. It was not feasible to distribute the external restraining forces on the specimens to be restrained against warping in exactly the manner that the mutual forces between the two halves of the corresponding specimens were distributed. As shown in the Appendix, the method adopted was to support the specimen as a simple beam and to apply enough force at the quarter-points to prevent warping of the central half.

As discussed previously and as shown by Equation 19*, the amount of warping of a specimen free to warp is indicative of the non-uniformity of shrinkage tendency. From similar considerations it follows that the amount of moment necessary to prevent warping is indicative of the non-uniformity of stresses resulting from the non-uniformity of shrinkage tendency. Furthermore, the difference between the actual moment required to prevent warping and that computed from the amount of free warping, assuming no plastic flow, gives an indication of the distribution of plastic flow. The results for one of the four cements are shown in Fig. 26. The lower curves give the actual moment developed, M, divided by the section modulus, I/c, for beams of three different thicknesses. The upper curves show what the Mc/I would have been if the restraining moment had not produced plastic flow. The upper curves are obtained from the measured values of the warping tendency and Young's modulus of companion specimens. Young's modulus was determined from resonant frequency of vibration.

Stresses based on flexure formula. Since the ordinates in Fig. 26 are in terms of Mc/I, they represent the stress in the outer fiber according to the elementary flexure formula. According to the lower curves of Fig. 26 the computed stresses for the 1-in. specimens reached a maximum of 410 lb. per sq. in. by the end of the first day of drying. The computed maximum stress in the 3-in. specimen was 490 lb. per sq. in. and was reached in 14 days. The computed stress in the 6-in. specimens had reached 500 lb/in^2 after 36 days and the indications are that, had the test been continued, the computed stress would have reached a maximum of about 550 lb per sq. in. after about 100 days of drying. These computed stresses in the outer fiber, based as they are on the flexure formulas, are of course not the actual stresses. The actual stresses in the drying surface will build up very rapidly (see curve $y/b = 1.0$ in Fig. 12*) and

*See Part 1

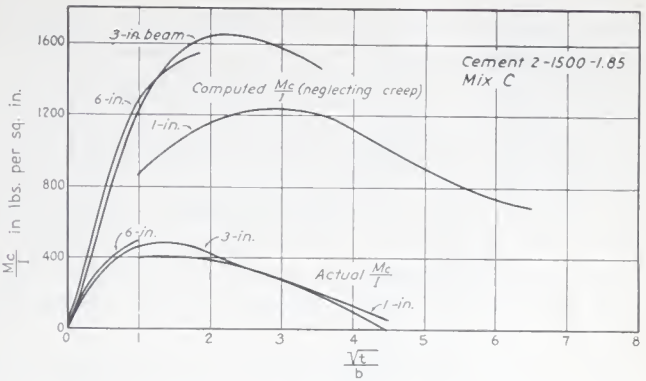

Fig. 26—Comparison of actual moment necessary to keep beams from warping with the conputed moment necessary to straighten companion beams that are free to warp. (Plotted in terms of $\frac{Mc}{I}$)

will build up as rapidly in the thicker slabs as in the thinner. The actual stresses are probably better represented by the solid curves of Fig. 27.

Stresses based on modified theory. The solid curves of Fig. 27 show stresses based upon a modified theory. These curves were obtained by substituting appropriate values of the parameters y/b, kt/b^2, fb/k, E, and S_∞ into Equation 20 of Part 1. For the construction of these curves the theory as presented in Part 1 was modified in that, instead of using constant values for the factors k, f, S_∞, and E, the following procedure was pursued:

(1) The ultimate shrinkage S_∞ was set equal to 750, 700, and 600 millionths, respectively, for the 1-, 3-, and 6-in. thick specimens. The selection of these separate values rather than one value for all specimens was governed by the apparent ultimate unit shortenings of the corresponding free-shrinkage specimens (Fig. 22).

(2) The ratio f/k was set equal to 2.5 in.$^{-1}$, i.e., fb/k was 2.5 for 1-in., 7.5 for 3-in. and 15.0 for 6-in. specimens. When this value of f/k and the above values of S_∞ were used, the theoretical maximum values of warping as given by curve A of Fig. 14* were found to be in agreement with the experimental values of maximum warping for each of the three thicknesses of specimens.

(3) A value of kt/b^2 was selected for each period of drying (1, 7, and 28 days) and for each thickness of specimen, such that when substituted along with the above values of S_∞ and f/k in Equation 23* for warping the result would be in agreement with the experimentally determined values for these periods and these thicknesses.

(4) A value of E was selected for each period of drying and each thickness of specimen such that the theoretical moment given by Equation 27 would be in agreement with the experimentally determined values.

*See Part 1.

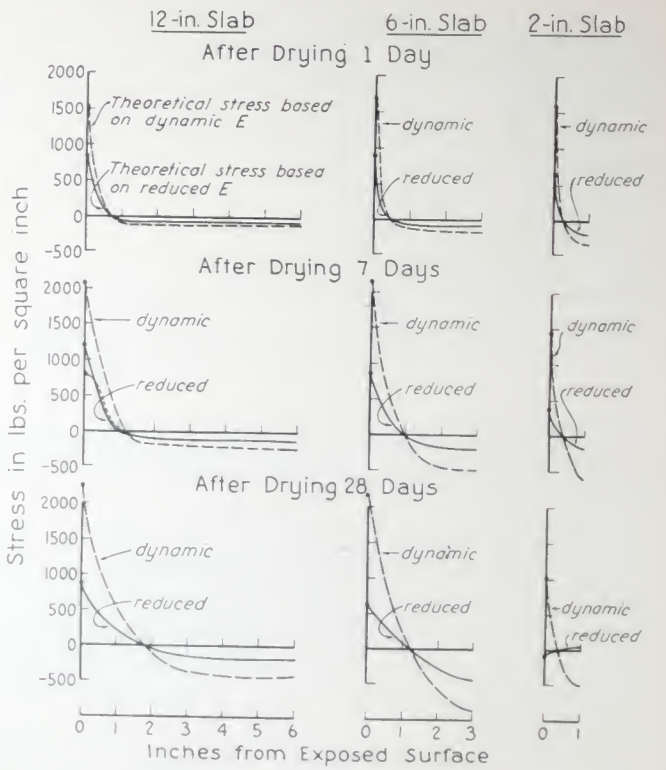

Fig. 27 Theoretical distribution of shrinkage stresses (modified theory) in slabs drying from two opposite surfaces for various drying periods and slab thicknesses

(5) The above values of S_∞, kt/b^2, fb/k, and E together with appropriate values of y/b, were substituted into Equation 20* and computations made for stresses. The solid curves were plotted from these computed stresses.

The dashed curves show the stresses that are obtained when the foregoing procedure of computing stresses is used except that the dynamic modulus of elasticity is used for E. The difference in the curves is a measure of the relief of stress by plastic flow and thus is a measure of the amount of plastic deformation that has occurred.

Although it is believed that for the most part the magnitude and distribution of stresses after the various periods of drying and for the various thicknesses of specimens are about as given by the solid curves of Fig. 27, the curves are probably in error in certain respects. The principal source of error lies in the assumption that the effects of plastic flow can be taken into account by using a reduced modulus of elasticity as is done when Equation 20 is used. Inelastic deformation is cumulative and depends on the past stress-history, not necessarily on the

*See Part 1.

stress at the moment. Furthermore, as explained in the section on plastic flow, the rate of flow for an element will depend on the rate at which the element is tending to shrink and may not be proportional to the stress on the element. Therefore, near the drying surface, where the stress has been relatively high from the beginning of drying, the plastic flow will be greater and the stress will be less than that indicated. Slightly farther inward where the stress has only recently changed from compression to tension the resultant plastic deformation will be less and the stress more than that indicated. The dotted curve in the one diagram of Fig. 27 represents an attempt to show a better estimate of the actual stress.

Reversal of stress by plastic flow. Fig. 26 indicates that eventually the stress in the outer fiber will become negative, i.e., compressive. In all restrained-warping tests that were continued until equilibrium of moisture content was nearly reached, the moment required to prevent warping decreased to zero and would have then become negative if restraint against negative warping had been provided. This means that when a wall dries from two opposite sides or a prism dries from all four sides, eventually the outer shell will be in compression and the inner core will be in tension.

Of interest in this connection is the fact that specimens of neat cement bars have been known to break spontaneously and audibly while resting in place in a storage rack. The explanation is that during the early part of drying large tensile stresses developed in the outer shell. As a result the outer shell was first permanently elongated and then caused to fail in tension, i.e., to crack. As drying proceeded inward, the inner core, which had not yet been stretched, tended to become shorter than the outer shell. The cracks closed, compression developed in the outer shell, and tension developed in the inner core. In some cases this tension was sufficient to cause failure of the core. A specimen would break spontaneously when failure of the inner core occurred at a section where the outer shell was already cracked.

Investigation of properties of concrete by means of slabs or prisms drying from one side only

As the foregoing has indicated, results from prisms drying from only one side have been very valuable for ascertaining in what ways the theory of diffusion is applicable to shrinkage of concrete. They are also valuable for investigating certain properties of concrete, especially if used in connection with the diffusion theory. The chief advantage of drying a prism from only one side is that it tends to warp as well as shorten as it dries and thereby makes possible measurements not obtainable on prisms drying from all surfaces.

As explained previously, the results from prisms drying from only one side indicated a cause for concretes of higher alkali content to show a greater tendency to crack under some conditions. Additional results in regard to fineness of grinding and percentage of gypsum will now be reported for the information they give to illustrate how such prisms may be used to investigate properties of concrete.

Effect of finer grinding on plastic flow. As explained previously, in addition to the one cement represented in Fig. 26 and 27, three other cements were tested at the same time and in the same manner. The results for the other cements were similar in most respects to those shown in Fig. 26 and 27 for the one cement. There were some differences, however. More plastic flow occurred in the specimens made with the two finer-ground cements. The differences in plastic flow with fineness of grinding in this test were similar to and in agreement with the differences shown for these cements in the restrained-shrinkage test (Fig. 25).

The effect of finer grinding on strength is similar to that produced by longer curing and therefore since longer curing decreases plastic flow we might expect that finer grinding would also decrease plastic flow. However, several cements tested in this way all showed that finer grinding increased plastic flow for both restrained-shrinkage and restrained-warping specimens. Other tests in this laboratory indicate that this effect of finer grinding on plastic flow is indirect. A given quantity of gypsum added at the time of grinding is less effective in retarding the early chemical reactions the finer the cement.[24] Lack of proper retardation of the early reactions because of insufficient gypsum results in a concrete of greater shrinkage tendency and greater capacity for plastic flow. Therefore, according to the indications, finer grinding, if unaccompanied by increase in percentage of gypsum, indirectly produces a concrete of greater tendency to deform inelastically.

This still leaves unanswered the question introduced in the discussion of Fig. 22 as to why the effects of plastic flow did not also reverse the relative positions of the curves for the finer-ground cements. Possibly at the very beginning of drying the coarser-ground cements, because of their relatively low strength, flow more readily but become less plastic than the finer-ground cements at the later ages when the strengths are more nearly equalized. However, since only slight differences in the way the different concretes deviate from the theory could account for the results and since concrete deviates from the theory in many different ways there are other possible answers to the question.

One possible answer is suggested in Fig. 24, according to which coarser grinding resulted in greater negative stresses at the end of the curing period. These negative stresses were produced by the tendency of the

concrete to expand during curing, especially the tendency to expand after some resistance to plastic flow had developed. Any tendency for the interior of the free-shrinkage specimens to continue expansion after the surface begins to dry would reduce the rate of shortening at the beginning of the drying period. If, as seems quite probable, this tendency is greatest for the thicker specimens with the coarser-ground cements, then these specimens would shorten relatively less at the beginning of drying than would be indicated by theory.

Effect of added gypsum. The effect of the gypsum in the cement on the properties of the hardened concrete was observed in an investigation in which 21 cements were made from the five clinker compositions listed in the Appendix. By blending various grinds of these clinkers, cements of different finenesses and different gypsum contents were obtained from each clinker. Concretes (Mix C) made from these 21 cements were tested in the manner indicated previously for prisms drying from only one side. However, in this investigation only the 3-in. size of specimen was used.

Where the C_3A content of the clinker was moderate or relatively high, an increase in SO_3, content decreased shrinkage and warping and also decreased plastic flow. Where the C_3A content was low, an increase in SO_3 had relatively little effect. According to other data obtained in this laboratory, a still further increase in SO_3 would have increased the shrinkage.[24] Representative results for a cement of high C_3A content are shown in Fig. 28, 29, and 30. As shown by Fig. 28, the maximum warp of those specimens free to warp was reduced appreciably by increase in per cent of SO_3. The reduction in shortening with increase in SO_3 agrees with that reported previously by other investigators[21, 24, 25].

Fig. 29 shows that the restraint developed by the specimens restrained against warping was in general less with the higher percentages of SO_3. However, increasing the SO_3 from 1.5 to 2.4 per cent had only a very small effect on the amount of restraint developed in the restrained specimens compared to the effect on the warping of unrestrained specimens. The explanation is that although the increase in SO_3 reduced warping it also reduced the tendency to yield under stress. The net result is some reduction in stress but not as much as would be anticipated from the results of the free-warping specimens.

Fig. 30 shows the effect of SO_3 on the factor of safety against cracking as determined by this test of a cement of high C_3A.

SUMMARY AND CONCLUSIONS

The theory that shrinkage of concrete follows the laws of diffusion similar to those followed by the flow of heat is tested by means of specially

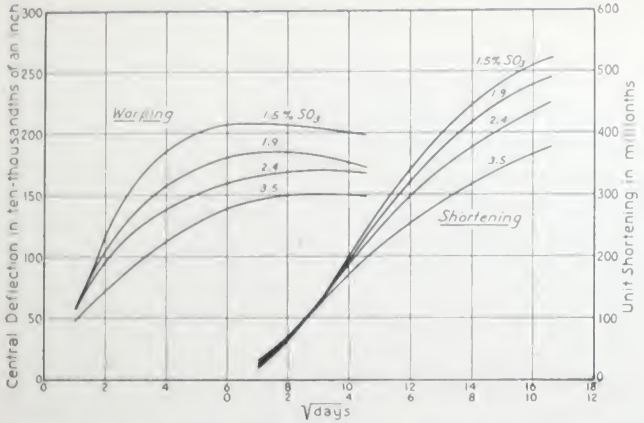

Fig. 28—Effect of gypsum on warping and shortening for a cement of high C_3A content

Cement from Clinker No. 1. Specific Surface 2100. Specimens 2 x 3 x 34-in. Cured 7 days. Sealed on all but one 2 x 34-in. surface. Central deflection over a 32-in. span.

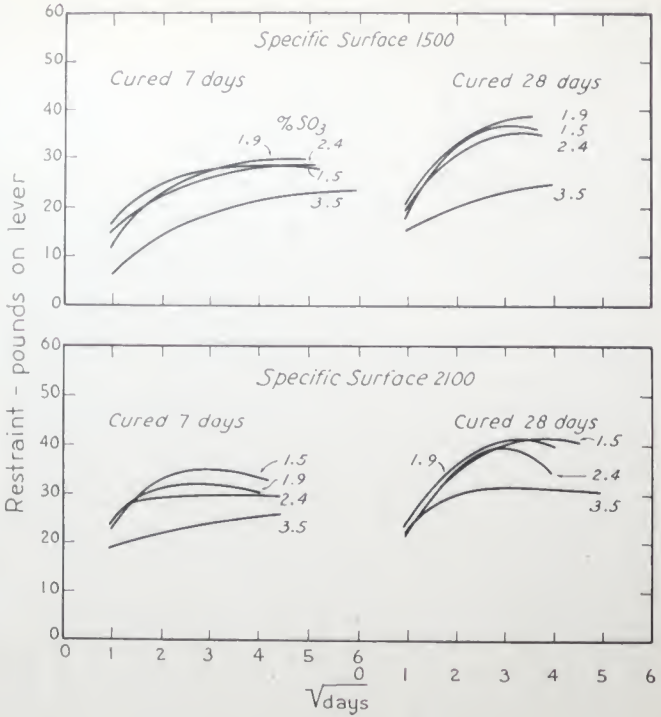

Fig. 29 (right)—Effect of gypsum, period of curing, and fineness of grinding on restraint necessary to prevent warping

Cement from Clinker No. 1. Mix C. 3-in. beams $\frac{Mc}{I} = \frac{32}{3}(W + 4)$ where W is pounds on lever.

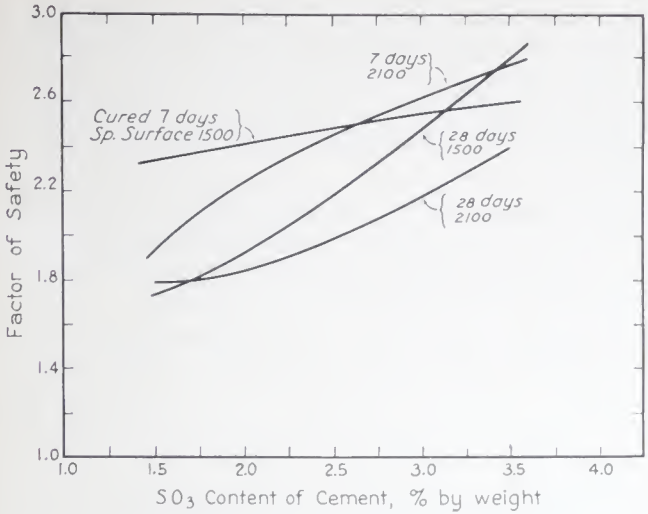

Fig. 30 — Effect of gypsum, period of curing, and fineness of grinding on factor of safety against cracking

Specimens same as those represented in Fig. 29.

designed experiments. According to the theory that was developed in Part 1, the shrinking and development of stress in a given concrete under given conditions of drying is considered to be characterized by certain constants. These constants are diffusivity of shrinkage, surface factor, ultimate shrinkage, and Young's modulus of elasticity. Equations were derived in Part 1 giving shortening and warping of prisms versus period of drying in terms of these constants and the dimensions of the prisms.

In Part 2 it is shown that these constants can be selected so that the shortening of a prism as computed by the theoretical equations is in good agreement with experimental values of shortening. Furthermore, it is shown that by using the same constants the shortening versus period of drying of other prisms differing in size and number of sides exposed to drying can be predicted with fair accuracy if the difference in size is not too great. However, it is shown that the theory must be modified to take into account inelastic deformation and to permit the supposed constants to vary with moisture content and size of specimen if the theory is to be in agreement with all results on all types of specimens of a given concrete.

The theory is used to explain various things about concrete; in fact, paradoxically, it is used to explain some of the ways in which concrete does not perform as predicted by the theory. The tendency of large specimens to crack more and shrink less than smaller specimens and the effect of alkali content of the cement in increasing the tendency to warp while reducing the rate of shrinkage are explained on the basis of the

theory. It is shown that when a saturated specimen is dried at 50 per cent relative humidity the stress developed would be much greater than the strength of the concrete if it were not for the effects of plastic flow. It is further shown that when a specimen is restrained against deforming the restraining forces are much less than they would be if plastic flow did not occur.

An example is given of the use of the theoretical equation in determining the distribution of stresses at various times during the drying of a specimen. In this example, consideration is given to plastic flow and to the decrease in diffusivity of shrinkage as the specimen dries.

The restrained-shrinkage test and the restrained-warping test are used to determine a factor of safety against cracking for concrete under conditions of drying and of restraint comparable to those under which the tests are made. These tests, together with tests on free-shrinkage and free-warping specimens, are used to measure plastic flow.

The various tests described in Part 2 and in the Appendix to Part 2 when used in conjunction with the theory given in Part 1 provide a means for studying some of the more fundamental properties of concrete and for predicting the performance of concrete under some conditions in the field.

ACKNOWLEDGMENTS

This paper developed during a study of the causes and the control of cracking of concrete. The author is indebted to many present and past workers in this field. E. A. Ripperger, now Lt. (j.g.) U.S.N. with the Pacific fleet, was responsible for a large part of the experimental work reported herein. He designed (or adapted from earlier designs) most of the special equipment used and was engaged in certain phases of the study previous to the author's participation. All of the work was done under the supervision of F. R. McMillan, Director of Research, and T. C. Powers, in charge of Basic Research.

The author is particularly indebted to Mr. Powers for assistance in preparing the manuscripts. His suggestions in regard to presentation of material and the wording of various paragraphs have been invaluable.

The author also wishes to thank Miss Adele Scott for preparing the diagrams and Miss Virginia Atherton for proofreading the manuscript.

APPENDIX TO PART 2

Mix proportions

Materials	Parts by Weight		
	Mix A	Mix B	Mix C
Water, net	0.5	0.355 to 0.388	0.487
Water added for absorption	...	0.048	0.083
Total water	0.5	0.403 to 0.436	0.570
Cement	1.0	1.0	1.0
Pulverized silica	0.6	....	....
Elgin sand	...	1.28	2.43
Elgin gravel (⅜" max. size)	...	1.82	2.97

Consistency

Consistency of Mix B with different cements was maintained fairly constant at from 5 to 6 in. of slump with a 12-in. cone by varying the amount of mixing water. The consistencies of Mixes A and C were allowed to vary with the different cements. Mix C usually gave a slump of from 2 to 4 inches, but with some cements the slump was as little as 1.5 inches and with others as much as 6 inches.

Materials

Cements: One cement designated M was a mixture of four brands of Type I cement, purchased in Chicago. Its specific surface by the Wagner method was 1665 sq. cm. per g. The other cements were prepared from five different commercial clinkers. From each of these clinkers cements of three different finenesses, coarse, medium, and fine, were prepared by grinding at the plant. In addition, two cements, one of low and one of high gypsum content, were prepared from each clinker by grinding in a small laboratory ball mill. The purpose in preparing these five different cements from each clinker was to make it possible to obtain any desired fineness and gypsum content by blending different grinds of the same clinker. In referring to these cements in the text the first number in the designation is the clinker number, the second is the Wagner specific surface, and the third is the per cent SO_3 content by weight.

The chemical compositions of the five clinkers and of cement M are shown below.

Oxides	Cement Clinker No.					Cement M
	1	2	3	4	5	
	Chemical Analysis, per cent by wt. (corr. for minor components)					
SiO_2	21.54	20.67	23.05	27.82	22.56	21.25
Al_2O_3	6.52	5.48	4.14	1.93	5.00	5.98
Fe_2O_3	1.56	2.50	4.35	1.87	2.48	2.69
Combined CaO	64.32	65.00	64.28	65.38	64.06	62.56
MgO	2.17	1.31	1.36	1.75	3.35	3.04
SO_3	0.41	0.19	0.03	0.17	0.20	1.75
Loss on Ign.	0.15	0.85	1.05	0.26	0.37	1.13
Free CaO	0.98	2.71	0.73	0.23	nil	0.79
Na_2O	0.17	0.30	0.05	0.05	1.13	0.28
K_2O	0.16	0.40	0.17	0.22	0.44	0.63
Compounds	Computed Compound Composition per cent by wt.					
C_3S	50.73	66.57	52.37	38.58	51.61	44.15
C_2S	23.49	9.05	26.58	50.66	25.75	27.62
C_3A	14.72	10.29	3.61	1.95	9.06	11.30
C_4AF	4.75	7.61	13.24	5.69	7.55	8.19

Aggregate: Sand and gravel were from Elgin, Illinois. The gravel was screened to pass a ⅜-in. sieve and be retained on a No. 4 sieve.

The sand was graded as follows:

Sieve No.	Per Cent Passing
100	5
48	15
28	43
14	67
8	82
4	100

Pulverized Silica: The silica was from the same source as standard Ottawa sand, but ground to cement fineness. Its specific surface by the air-permeability method was 3200 sq. cm. per g.

Procedure

With some exceptions the procedure in preparing and testing the specimens was as follows:

Preparing the specimens: The materials were mixed in a power-driven open-tub mixer. The fractions of the various-sized aggregates and grinds of cement were weighed and placed in the tub. The mixing schedule was: mix ½ minute dry, 2 minutes wet, rest 3 minutes, mix 2 minutes. (Special tests showed that the grinds of cement were adequately blended in ½ minute of dry mixing in the presence of sand.)

The freshly mixed concrete was placed in steel molds and consolidated by light vibration by placing molds on a platform-type vibrator. Covers were fastened on the molds but not made water-tight. Each mold was equipped with restraining bars, gage inserts, etc., the details of assembly depending upon the tests to be made.

The molds and contents were stored under water at 74 F for one day. The molds were then stripped and the specimens returned to water at 76 ± 1 F in a covered tank where they were left for one hour. The specimens were then removed one at a time, dried with a cloth, and all initial measurements of length, deflection, and weight were made. All dimension measurements were made within 30 seconds after removal from water, and weighings were made as soon thereafter as practical. The specimens were then returned to the 76 F curing tank.

One day before the end of the curing period the specimens were removed for sealing of certain surfaces against the loss of moisture. The surfaces to be sealed were wiped with a cloth and then allowed to air-dry until the surface *just* changed color. During this time, scheduled measurements were usually made. After the color change and before any appreciable loss of moisture by evaporation, one coat of black, quick-drying brushing lacquer was applied. After the lacquer had dried a few minutes, the excess was removed with a cloth and one coat of hot paraffin was applied to the lacquered surface. While a second coat of paraffin was being applied, one thickness of newspaper of appropriate shape was pressed into the still soft paraffin somewhat in the manner in which a paper hanger applies wallpaper. Next, a final heavy coat of paraffin was applied. The layer of paper helped to eliminate pin holes. (When only the ends of prisms were sealed, the paper and final coat were omitted.)

After the specified surfaces were sealed, the unsealed surfaces and exposed steel parts were cleaned, vaseline was applied to the steel parts, and the specimen was returned to the curing tank for an additional day of curing. At the end of the curing period the specimens were transferred from the curing tank to a room maintained at 76 ± 1 F and

50 ± 2 per cent relative humidity. At this time the vaseline was removed from the steel parts and measurements for the beginning of the drying period taken.

Testing the specimens: The testing was considered to have begun in most of the tests with the beginning of the drying period. The specimens may be divided into classes, according to the tests made, as follows:

Free shrinkage specimens were measured for length changes, weight losses and resonant frequency of vibration. Reference plugs were cast in the ends of the specimens for the length-change readings. They were hex-head cap screws arranged to give the desired gauge length. Ordinarily these were single plugs centrally located in the ends. But for those prisms that represented slabs drying from two opposite sides the arrangement was as shown in Fig. 31.

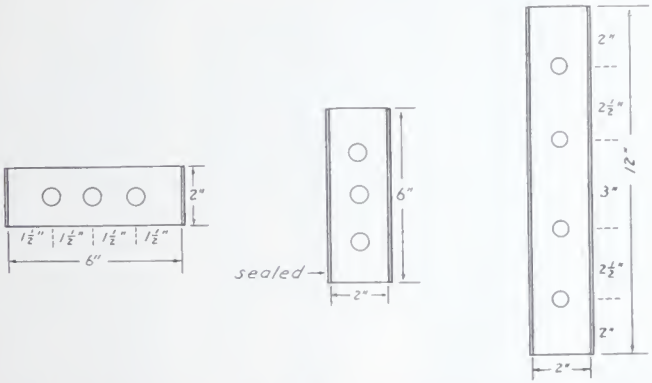

Fig. 31—End views showing arrangement of gage plugs in specimens representing 2-in., 6-in. and 12-in. slabs

The gage plugs for these specimens were ⅜ in. bolts 4 in. long.

Restrained shrinkage specimens were partially restrained against shrinkage by steel restraining bars. The arrangement of the bars in those specimens that represented slabs drying from two opposite sides was the same as that shown in Fig. 31 for gage plugs except that only two bars 3 inches apart were cast in the 2x6-in. specimens. Square specimens that are permitted to dry from all four sides and that are partially restrained by one centrally located bar are used in routine testing of resistance to cracking. Further details in regard to restraining bars and the measurements for change in length of the restraining bar are shown in Fig. 32 and 33 as well as in Fig. 23 body of the text.

If the restrained-shrinkage specimen did not crack spontaneously before the maximum restraining force had been developed, additional increments of load were applied as shown in Fig. 33 until failure was produced.

Free warping specimens were measured for deflection over a 32-in. span. Most of these specimens were also measured for length change, weight loss and resonant fre-

quency. Some of the free warping specimens made in the early part of the work were not equipped for length-change measurements. Cross sections of free warping specimens are shown in Fig. 34. See Fig. 35.

Restrained warping specimens companion to the free warping specimens were loaded, as shown by Fig. 36, so as to prevent warping between the loaded quarter-points. Readings of the load required were taken periodically and, after the maximum restraint had developed, the load necessary to produce failure was determined.

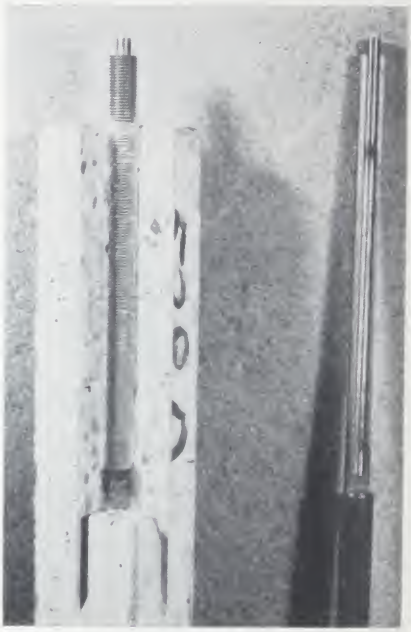

Fig. 32a (left)—Comparator
Fig. 32b (above)—Restraining Bar

Measurements of shrinkage-stress are made whether cracking occurs or not. The comparator (in Fig. 32a) is used to measure the changes in length of the steel restraining bar that result from the strains placed on it by the concrete. From these measurements and the known properties of steel, the average stress in the concrete is computed.

Important details of the restrained-shrinkage type of specimens are shown in Fig. 32b (See also Fig. 23 in the text.) Note that the concrete can grip the bar only in the end-region; contact in the 20-in. central section is prevented by a thick layer of rubber.

Fig. 33a

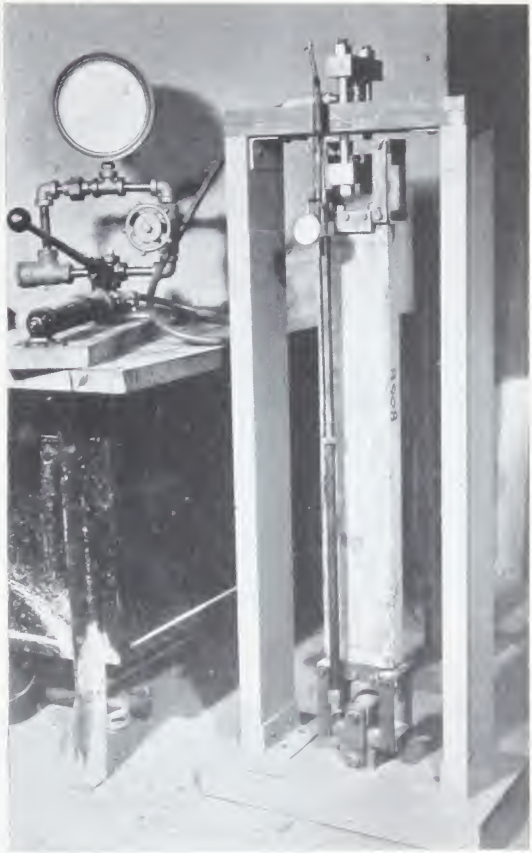

Fig. 33b

This method of test has been used to measure shrinkage-stress in specimens as wide as 12 in. and containing as many as four restraining bars.

Those specimens that do not fail under shrinkage-stress alone are given additional stress with the machines shown in Fig. 33a and 33b. The machine at the left (Fig. 33a) is used for most of the specimens; that at the right Fig. 33b is used if the capacity of the other one is exceeded and if the specimen contains more than one bar. The load is applied to the bar, and the extension of the bar at the time the concrete fails is determined by the strain-gage shown in the pictures. The net amount of load on the concrete at failure is computed from the magnitude of the load and the strain-gage reading. The factor of safety is the ratio of the load on the concrete at failure to the maximum load represented by the restraint against shrinkage.

"Sonic" testing: Most of the "unrestrained" specimens are tested periodically for frequency of vibration with the apparatus shown in Fig. 35a. Young's modulus is calculated from the resonant frequencies.

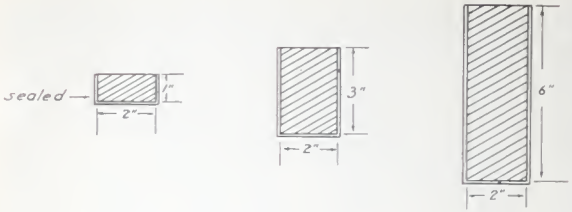

Fig. 34—Cross section of free warping specimens.

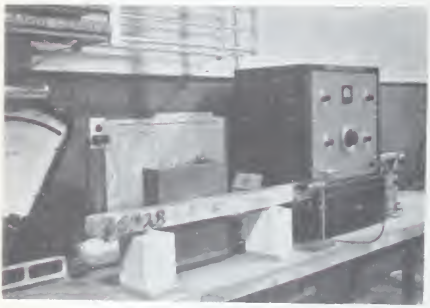

Fig. 35a—Sonic testing

Fig. 35b—Warping measurement

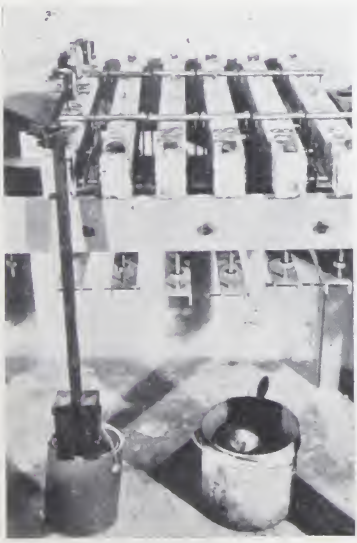

Fig. 36a (above)
Fig. 36b (left)
Restrained warping

Warping, length-change, and moisture-content: On specimens like that shown in Fig. 35a, the change in length is measured with the comparator shown in Fig. 32 and the warping is measured with the curvature-gage shown resting on a specimen in Fig. 35b. Results are correlated with concomitant changes in moisture-content.

Warping due to swelling: Previously dried specimens are placed, uncoated side down, in a trough of water as shown Fig. 35b or they are exposed to saturated air. The resulting warping due to absorption at one surface is more rapid than that due to shrinkage and can give rise to larger stresses.

The specimens shown Fig. 36 are supported only at the ends. They are coated on all but the bottom side and therefore as they dry they tend to bow upward. This tendency is opposed by the shackles at the quarter-points which are connected to a lever system below, one for each specimen. The levers are held by the fine-thread screw-adjustment seen best in Fig. 36b. The screws are turned downward until the force is just sufficient to prevent warping as indicated by the curvature-gage shown in both pictures. This instrument can be moved from specimen to specimen.

The force on the lever is measured periodically by finding the weight (bucket of shot) that will just hold the specimen in the position maintained by the screw. The force required reaches a maximum and then recedes slowly to zero as drying continues. When the maximum is reached, the specimens are loaded to failure. The ratio of the maximum force required to prevent warping to that required for failure is the factor of safety.

This test gives approximately the factor of safety against cracking of slabs of twice the depth of the specimens, drying equally from both sides.